ALMA MATER STUDIORUM
UNIVERSITÀ DEGLI STUDI DI BOLOGNA

Scuola di Ingegneria e Architettura
Corso di Laurea Magistrale in Ingegneria Biomedica

MODELLING, SIMULATION AND CHARACTERIZATION OF EPITHELIAL CELL CULTURE BIOCHIP

Elaborata nel corso di: Sensori e Nanotecnologie

Relatore:
Prof. MARCO TARTAGNI

Candidato:
ANTONIO CANDITO

Correlatori:
Prof. HYWEL MORGAN
Ing. RICCARDO REALE

ANNO ACCADEMICO 2013–2014
SESSIONE III

PAROLE CHIAVE

Organ-on-Chip
Tight Junctions
Double Layer Effect
Impedance
Lock-in Amplifier

Contents

Introduction **ix**

1 Epithelial Cell Culture Biochip **1**
1.1 Organ-on-chip 3
1.1.1 State of the Art 3
1.2 Microfluidic device 8
1.2.1 Microfluidic device structure 8
1.2.2 Experiment Workflow 9

2 Modelling and Simulation **11**
2.1 Equivalent circuit model 11
2.1.1 Parameters of the model 15
2.1.2 TEER measure with Chopstick-type Electrodes 17
2.1.3 Cells Resistance 18
2.2 Reagents 19
2.3 Matlab Simulations 19
2.3.1 Frequency Input Signal 22

3 Biochip Characterization **23**
3.1 Double layer 23
3.1.1 Double layer Model 24
3.1.2 Electrical Double Layer Effect 28
3.1.3 Electrodes Biochip 32
3.1.4 Electrochemical deposition of Pt black 34
3.1.5 Impedance response of Pt black coated electrodes 37
3.2 Spectroscopy of Impedance 41
3.2.1 Alpha-A Analyzer Novocontrol 42

3.2.2 Biochip impedance to Check the Electrical Double Layer Effect 43
3.3 Impedance Measurement with Novocontrol 45
3.3.1 Experimental Measurement of the Biochip Impedance 45

4 System Instrumentation 61
4.1 Lock-in Amplifier 61
4.1.1 Phase-Sensitive Detection 62
4.1.2 Narrow Band Detection 65
4.1.3 Magnitude and Phase 65
4.2 Complex Impedance Detection by Lock-in 67
4.3 Noise Sources 69
4.3.1 Johnson Noise 69
4.3.2 Shot Noise 69
4.3.3 Flicker Noise 70
4.4 PCB Design 70
4.4.1 PCB Routing 70
4.4.2 Working Principle 74
4.4.3 Lock-in Amplifier Simulation 78
4.4.4 Matlab Script 89
4.5 Chip to World Connection 90
4.5.1 Design 90

5 Conclusions 93

Appendix 1 95

Appendix 2 99

Appendix 3 103

Appendix 4 107

Appendix 5 109

Acknowledgements 119

Introduction

Asthma is a medical condition which leads to symptoms like cough, wheezing, chest tightness and breathlessness. Its symptoms can range from mild to severe as they show big variations among different patients. Sometimes People affected undergo a temporary significant worsening of the symptoms which require medical assistance and that can lead to life-threatening conditions.

As of now, 5.4 millions of people in the UK (making up the 8.3% of the adult population and the 9.1% of the children population) are affected by asthma [1].

The annual cost of asthma for the society has been esteemed to be more than £1 billion in the UK [2]: among these, there is a component of direct costs (i.e. medical expenses for the care of patients), and one of indirect costs (i.e. absence from workplace and school) of the disease.

The cell barrier that protects the inner part of the lungs from external toxicants plays an important role in this disease. This cell layer is called airway epithelium. This cell layer in addition to ensure the passage of substances essential for the proper functioning of the organ, plays a role in the defense against pathogens agents such as bacteria. If bacteria run over this barrier they can cause inflammation of the lungs that can lead to disease such as asthma. The bronchial epithelial cells layer is kept together by proteins amount which the most important are ones that form the tight junctions.

The tight junctions are intracellular areas which are almost impermeable due to the presence of strong bonds between the two cells. The bonds between the cells are formed by membrane proteins as occludin and claudin.

It has been clinically observed that in patients with asthma the

tight junctions are disrupted, leading to an increased permeation of exogenous agents in the endothelium.

A microfluidic device was to propose to study the changes chemical and the electrical properties of epithelial cells. In particular, the goal of this microfluidic device is to recreate physiological conditions for the differentiation of the cells so that it is possible to culture them for long period and to challenge them with inflammation stimuli.

When an inflammation occurs the epithelial cells lose the barrier function because the tight junctions are destroyed. When the cells express the tight junctions proteins the electrical resistance of the layer is increase.

To monitor the barrier function of the epithelial cells the magnitude and phase of the layer's impedance were measured. On the device there are electrodes that will measure a current signal when a potential dif- ference is applied between them. This signal will depend on impedance of the cells monolayer. The output signal from the biochip is processed by an electronic circuit that allows to measure the impedance of the epithelial cells monolayer. The objective of the thesis is to develop an electronic circuit that allows measurements of the biochip impedance.

The system was modeled as an Equivalent Circuit model. The Equivalent Circuit Model allows to estimate the values of magnitude and phase of the monolayer at different frequencies and to understand if the cells are healthy or not.

By simulating the biochip the frequency of the stimulus signal was chosen. The frequency chosen 300Hz. However at this frequency the problem of double layer effect emerged. To solve this problem an electrochemical deposition of black platinum platinum electrodes was performed, so that there will be an increase of the area of the electrodes and the double layer will no longer dominate at low frequencies. The decrease of the double layer effect was evaluated with measures of impedance using an Impedance Analyzer, comparing the measurements of coated and uncoated electrodes.

After the modelling and the characterization of the biochip an electronic circuit that allows to measure the biochip impedance was designed.

The parameter used to provide the integrity of epithelial cells monolayer is the trans-electrical-epithelial-resistance or TEER.

The circuit chosen to measure the impedance was a Lock-in amplifier because it allows to measure small signal even in presence of greater source of noise. The project of the circuit was also aimed to build a low-cost system.

Chapter 1

Epithelial Cell Culture Biochip

The surface of the airways is exposed to air that contains dusts and microorganisms. These environment is a filter efficient and a defense mechanisms that prevents the development of an inflammation in the lungs. The first line of defense in the lower airways is provided by the bronchial epithelium which protects the inner part of the lung against inhaled agents.

The bronchial epithelium is formed by protein amount which the most important are the ones that form the tight junctions.

The tight junctions are proteins complex positioned between adjacent cells that regulate the transport through extra-cellular matrix. The tight junctions encircle the cells and stick to other near cells. These junctions act as a barrier for the molecules that diffuse across the epithelial through the adjacent cells. The tight junctions are the major regulator of permeability, expressing different levels of "tightness" based on location and chemical stimuli [3,4,5].

Technologically a measure of tight junctions tightness is used as a indicator of the health of the epithelium. This measurement is usually performed electrically, analysing the electrical properties of a confluent cell layer.

When the tight junctions are destroyed the barrier no longer protects the surface of the airways and maybe is crossed by bacteria and this can bring to beginning of diseases such as asthma. An example

of the differences in the structure of the tight junctions between an healthy epithelium and when a cell layer loses the barrier function is shown in Fig.1.1.

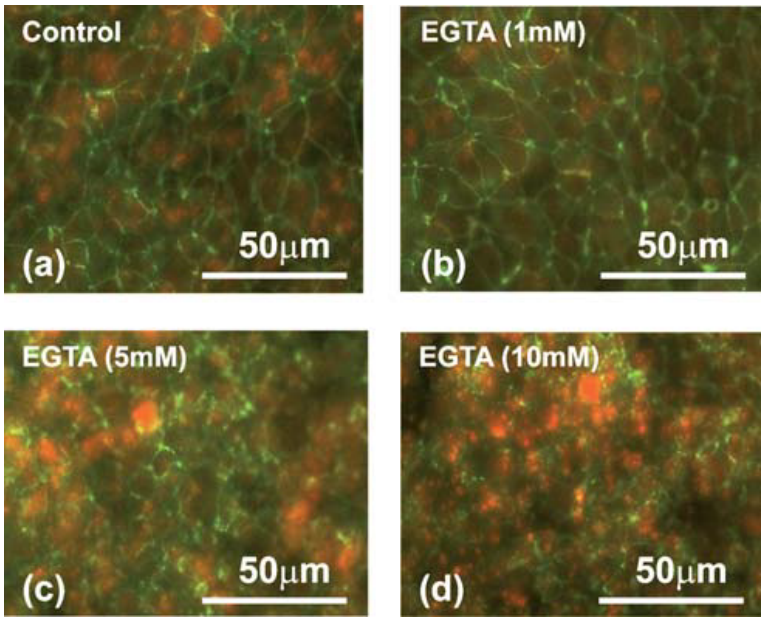

Figure 1.1: Images showing the immunofluorescent staining of the tight junction protein ZO-1 in the epithelial cell monolayers, treated with EGTA at the concentrations indicated. (a) Control cell monolayer, (b) 1mM EGTA treatment, (c) 5mM EGTA treatment, (d) 10mM EGTA treatment [6]

A microfluidics device that creates a physiological environment where the epithelial cells monolayer can be grown has been proposed. The cells are placed on the biochip where they can begin to differentiate as they are fed with medium. The physiological environment created by the microfluidic device allows to keep the cells alive for a long period. In this way we can study the behavior of epithelial cells monolayer when the cells are treated with reagents that destroy the tight junctions.

The project of the microfluidic device is based on a technology called Organ-on-Chip.

1.1 Organ-on-chip

Organ-on-chip are microfluidic devices used for cell culture. These devices are composed with of micromiter-sized chambers. In this chambers medium is pumped so that cells are continuously perfused. The simplest system is formed from a single chamber where there are only one type of cells. This system exhibits the functions of a single type of tissue. In more complex designs two or more micro chambers are connected with a porous membrane lined and different cell types are cultured to recreate interactions between different tissues. This systems are made by soft lithography, a means of replicating patterns into silicon chips in more biocompatible and flexible materials [7].

The microfluidic device allows for the control of parameters that are not easily controlled with 3D static cultures or bioreactors, facilitating the study of physiological phenomena. Microsensors that probe the cells culture conditions can be integrated in this device. These integrated microsensors serve to study the tissue barrier integrity, cell migration and fluid pressure.

1.1.1 State of the Art

We can summarize the state of the art of Organs-on-Chip with two previously published works. Those are the main work from which this project has been inspired.

The first work describes a Bio-impedance chip for the *in-vitro* real-time monitoring of the epithelial cells monolayer [6]. The goal of this work was to study the barrier epithelium cells monolayer. The barrier is formed from the tight junctions that seal together adjacent cells. The impedance of the barrier is commonly used an indicator for the presence of the tight junctions. The device is based on a Transwell.

The Transwell are a commercial support widely used for a static cell culture. They are formed with a polymeric support with a nano porous membrane glued on the bottom. They have an opening between the walls so that this design allow to insert electrodes to measure the TEER. They have a ridge in the top part which holds them suspended on a commercial wells plate.

The utilization of the Transwell as device for a cell culture static allows for a good differentiation of the epithelial cells so that they form a barrier with a good integrity.

The electrodes were integrated in a PCB which was used as support for the Transwell (Fig. 1.2).

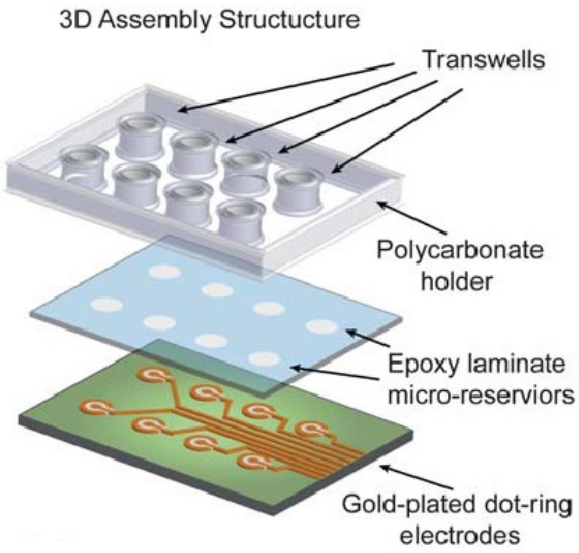

Figure 1.2: 3D assembly structure of the Bio-impedance chip [6]

The electrodes were gold-plated. To decrease the double layer effect the polymer polypyrrole (PPy) doped with polystyrene (PSS) was electrochemically deposited onto the surface of the electrodes.

The parameter used to characterize the integrity of the epithelium cells monolayer was the Trans-epithelial-electrical-resistance (TEER).

The cells were treated with reagents to recreate a physiological disease. The reagents were Triton X-100 and EGTA (ethylene glycol tetraacetic acid). These reagents destroy the tight junctions, leading to weaker links between the cells and thus to a lower impedance of the layer (Fig. 1.3).

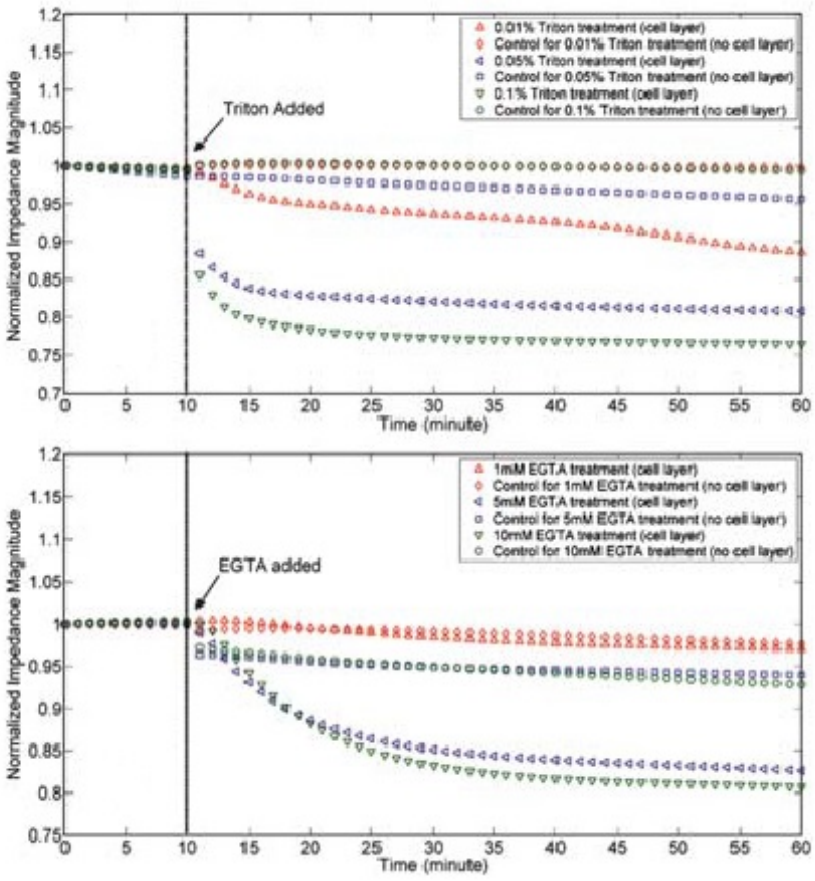

Figure 1.3: The cell monolayers were treated with different concentrations of TX-100 and EGTA. The data show the disruption in the epithelial cell barrier function [6]

The second work considers the issues that arise when TEER is measured in microfluidic systems, particularly when the results of these measurements are compared with values found in Transwell culture devices [8]. The device consists in two parallel channels separated by membrane with pores (Fig. 1.4).

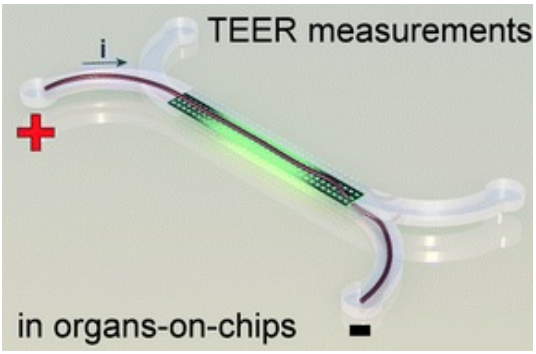

Figure 1.4: Organ-on-Chip [8]

A cell layer was cultured on the membrane and it was continuously perfused. This microfluidics is an example of Organ-on-Chip that allows for a dynamic culture. The goal of this work was to demonstrate that a dynamic culture allows to characterize the integrity of the epithelium cells monolayer more accurately than a static culture makes with Transwell. Analysis of the same human intestinal epithelial Caco-2 cells grown in both the Organ-on-Chip and Transwell revealed that the absolute TEER values measured in the Organ-on-a-Chip are consistently higher than those measured in the Transwell cultures (Fig. 1.5).

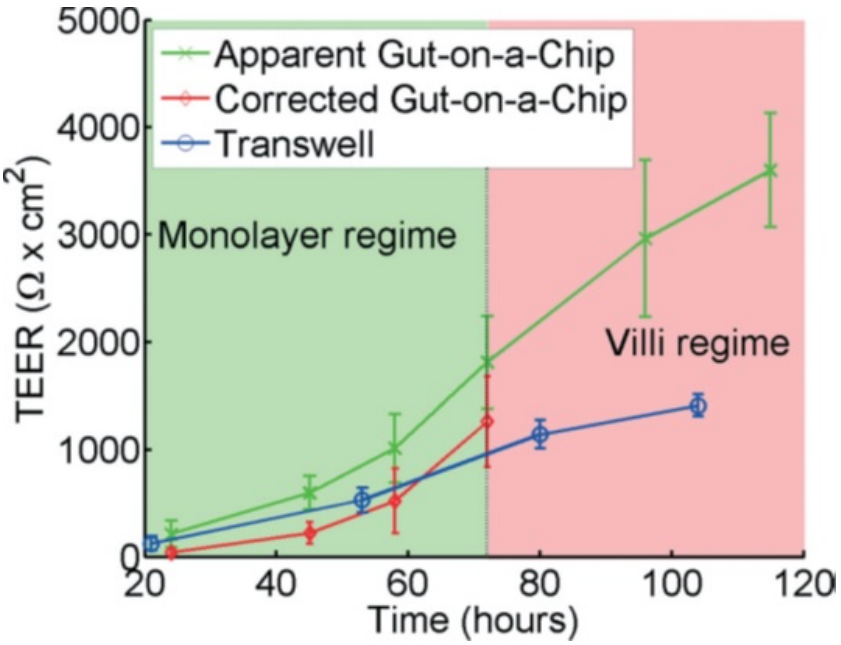

Figure 1.5: TEER measurements for the Organ-on-a-chip and Transwell using human intestinal epithelial Caco-2 cells [8]

The TEER values were measured with a multimeter, however a prolonged use of a single electrode would lead to undesired changes in resistance due to changes in the electrode surface. More over in this cases the TEER measurement is very sensitive to temperature variations.

1.2 Microfluidic device

The device proposed in this project allows for a dynamic cells culture. The measurements of the cells impedance to study the epithelium barrier integrity are performed with an electronic circuit in AC. The parameter to characterize the epithelium cells monolayer is the TEER. The electrodes are coated to decrease the double layer effect. A solution to the problem of temperature that can affect measurements of impedance is proposed.

1.2.1 Microfluidic device structure

The microfluidic (Fig. 1.6) device used to study of asthmatic bronchial epithelial cells is structured as follows:

- Glass as bottom layer
- Metal electrodes are deposited
- A channel is patterned using the standard photolithography process of a photosensitive polymer
- A hole is etched through the glass to define the outlet channel
- A membrane is placed on top of the electrodes as the support for the cells
- The bulk part of the device is placed on top. It needs an inlet channel and a seeding chamber
- Microfluidics port connect the inlet channel to the external world

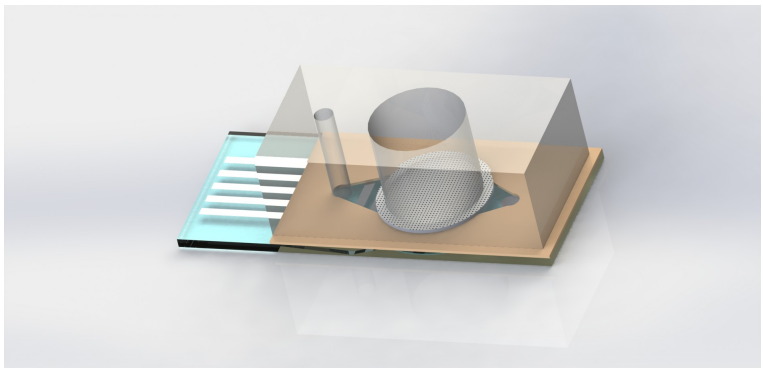

Figure 1.6: Microfluidics Design Biochip

1.2.2 Experiment Workflow

The observables that will be analyzed during the experiment are the chemical response (i.e. the amount of cytokines produced) and the electrical response of the cells (the Trans-membrane-impedance). The trans-membrane-impedance will be measured using the electrodes that are located under the membrane.

The workflow of a typical experiment is:

- The cells are seeded in the device and left to sediment and grow
- When they reach confluence, the acquisition of the measurements will start: a potential difference will be applied to the electrodes and the output will be measured.
- After the system has stabilized, the culture will be challenged with a stimulus as a reagents that destroy the barrier function of the cells monolayer. If the cells are affected by the stimulus, there will be a decrease of the cells impedance.

Chapter 2

Modelling and Simulation

The Equivalent Circuit Model allows to model the biochip as an electronic circuit and so that the electrical properties of the device can be characterized. By modelling the system it is possible to simulate the behavior of the biochip so that the variations of impedance at different frequencies can be estimated and the loss of the barrier function assessed. With the simulations of the biochip impedance is possible to choose the frequency for the stimulus signal.

The parameter that allows to understand when the cells are healthy or when they have lost the barrier function is the TEER. The TEER provides a measure of the integrity of the epithelial barrier and is generally performed using a hand-held TEER meter, in which pair of chopstick-type electrodes measures the resistance at low frequencies.

2.1 Equivalent circuit model

The biochip was designed with a part for the cell culture and with a part to measure the cells impedance. The cell culture part is composed by a channel for the medium flow and by a thin nano porous membrane. The medium flow through the channel filling the basolateral and the apical part of biochips as these two areas are fundamental for maintaining the cells alive. The part to measure the cells impedance is composed with two electrodes one being dot-ring the other being straight.

The working principle of the biochip is described in the figure 2.1. When a potential difference between the dot-ring electrodes is applied a current is generated. The measurements of this current give information on the cells impedance.

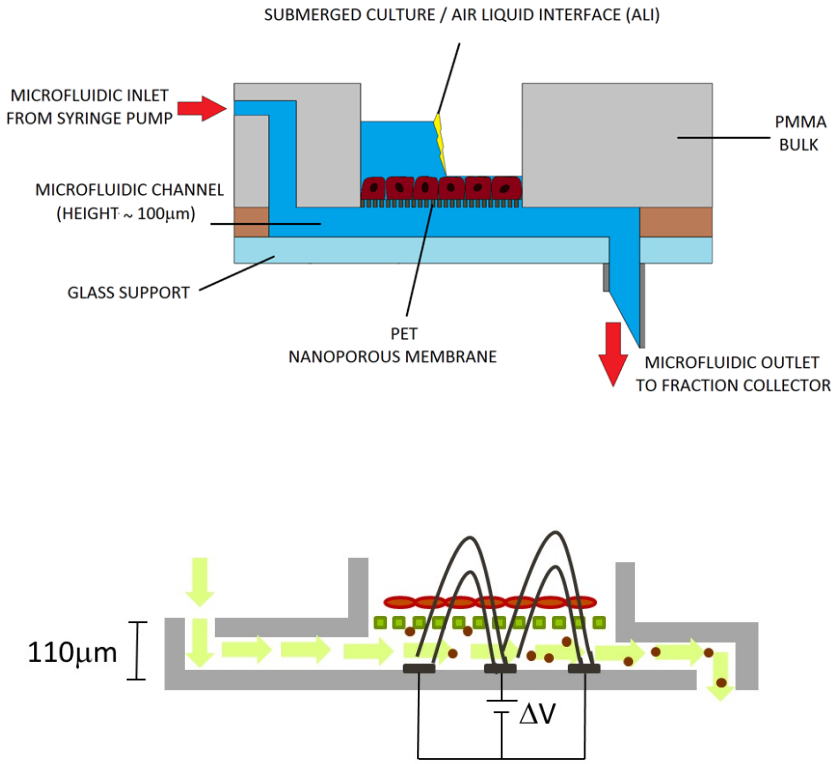

Figure 2.1: Epithelial cell culture Biochip

Every part of the biochip can be modelled as an element or combination of elements of an electrical circuit. Therefore by analyzing the electrochemical system as a circuit valuable information can be derived.

Equivalent circuit model provides a quantitative tool to analyze impedance data. Several circuit models have been proposed to extract the electrical properties of epithelial cell monolayers. The cells sit on the membrane and they are modelled as single particles connected by a tight junction with variable resistance and capacitance. The impedance of the electrical double layer, Z_{EDL}, is modelled as a constant phase element (CPE):

$$Z_{EDL} = [T(j\omega)^p]^{-1}; 0 \leq p \geq 1$$

where $i^2 = -1$ and the constant T is a combination of properties related to both the surface and the sample and it is independent of frequency. When p = 1, the EDL is purely capacitive and when p = 0, the EDL is resistive.

The impedance of the culture medium is modelled in three parts: basolateral medium (R_{bm}), medium in the nanopores (R_{tm} and C_{tm}) and apical medium (R_{am}). The impedance contribution from the epithelial cell monolayer is modelled as one part: the impedance of the cells (R_c and C_c).

The Equivalent circuit model of the biochip is shown in Fig 2.2. and the impedance of the system Z_{sys} is:

$$Z_{sys} = Z_{EDL} + \left(\left(\frac{R_{tm}}{1 + i\omega R_{tm} C_{tm}} + R_{am} + \frac{R_c}{1 + i\omega R_c C_c} \right)^{-1} + R_{bm} \right)^{-1}$$

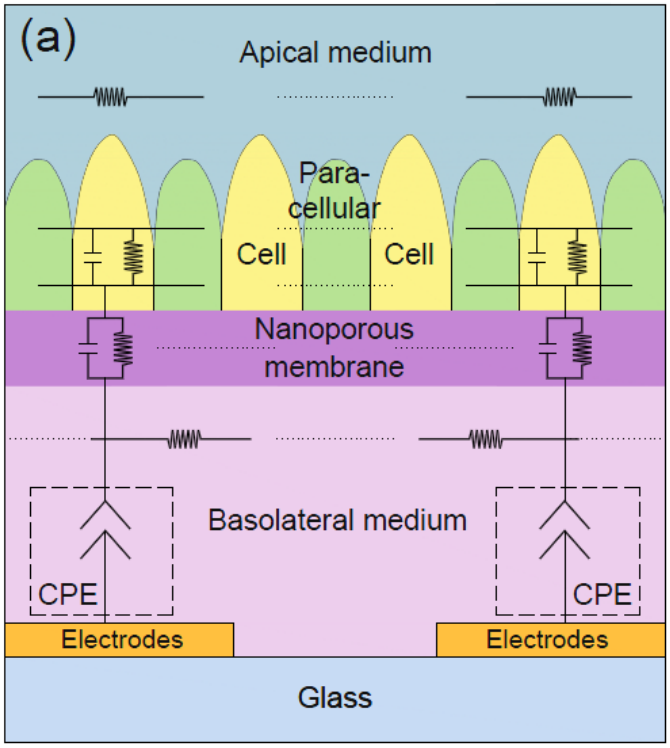

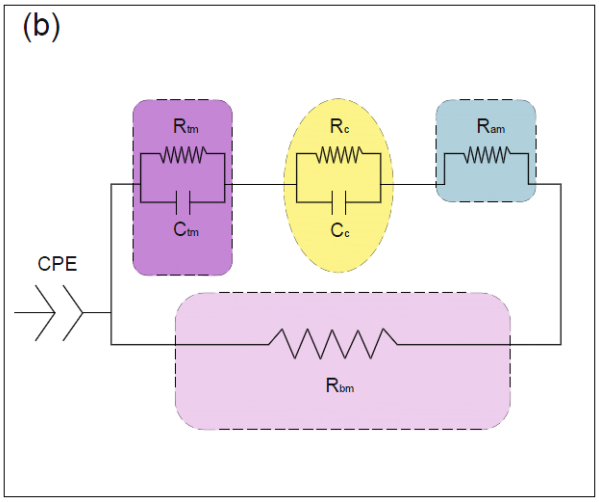

Figure 2.2: Equivalent circuit model of the system for extracting the electrical properties of the epithelia cell (a), (b) simplified model

2.1.1 Parameters of the model

The values of Rbm and Ram were calculated with the expression $\frac{K}{\sigma}$ where k is the cell constant and σ is the conductivity of the medium. The impedance values in the nano-pores were calculated based on the dielectric properties of culture medium and the geometrical configuration of pores (density, thickness and diameter of pores). The values of the EDL parameters were derived by fitting the impedance spectra of the circuit model to the measured impedance data using ZView (Scribner Associates Inc.). To extract the electrical properties of the cell layer, the parameters associated with the culture medium were assumed to be unchanged.

The values of these parameters were estimated with relations which depend largely by geometric factors but to estimate the values of the cells resistance and as they change the impedance when the cells lose their barrier function was used the definition of TEER.

The parameters for the biochip used in the model are the following:

$$\sigma = 1.47\frac{S}{m}$$

Resistance Basolateral medium:

$$R_{bm} = \frac{K_{Dot-Ring}}{\sigma(T)}$$

$K_{Dot-Ring}$: cell constant Dot-Ring electrodes
Resistance of the membrane:

$$R_{tm} = \frac{l_m}{A_{pores}\sigma(T)}$$

A_{pores}: area of the membrane pores
l_m: length membrane $= 12\mu m$
Capacitance of the membrane:

$$C_{tm} = \epsilon_0 \cdot \epsilon_{pet} \cdot \frac{A_m}{l_m}$$

ϵ_0: electric constant
Area Total membrane:

$$A_m = A_{pl} + A_{pores} = 0.19cm^2$$

A_{pl}: area where there are no pores:

ϵ_{pet}: relative dielectric constant of the polymer with which the membrane is made

Pore density:

$$\rho_{hole} = 4 \times 10^2 \left[\frac{holes}{cm^2} \right]$$

Pores diameter:

$$d_{pores} = 0.4\mu m$$

Area of a pore:

$$A_{hole} = \pi \frac{d^2}{4} = 0.125\mu m^2 \rightarrow 1.25 \times 10^{-9}$$

$$A_{pores} = \rho_{hole} \cdot A_{hole} \cdot A_m = 5 \times 10^{-3} = 1.17 \times 10^{-3} cm^2$$

$$R_m = 48\Omega$$

$$C_m = 97pF$$

$$K_{Dot-Ring} = \frac{\ln \frac{r2}{r1}}{2\Pi h} = 735m^{-1} \rightarrow R_{bm} = 500\Omega$$

r2: Dot radius

r1: Ring radius

h: height of the channel

Resistance Apical medium:

$$R_{am} = 189\Omega$$

R_{am} depends of the quantity of medium pumped into the apical region of the device

Capacitance of the membrane:

$$C_c = 1.26 \frac{\mu F}{cm^2}$$

2.1.2 TEER measure with Chopstick-type Electrodes

The method most used to measure the TEER provides using of chopstick-type electrodes. A pair of chopstick-type electrodes is formed with two metallic (Ag/AgCl) pads placed on the tip of two electrodes. The procedure provides that a stick is placed on the apical part, where the cells and the membrane are placed, while the other stick in the basolateral part.

The measurements depend from the positions of the electrodes due to non uniform distribution of the current. This can cause systematic errors in the measurements [9, 10].

In Fig. 2.3 we can see a example of chopstick electrodes and Transwell.

Figure 2.3: Chopstick Electrodes and Transwell

2.1.3 Cells Resistance

The values of the cells resistances were estimated with the use of TEER.

A current is generated when a small AC voltage is applied. The current will be measured by a I/V convert that will give a value of the resistance based on the current value.

The value of TEER depends on the contribution of the apical medium resistance, of the basolateral medium resistance, of the membrane resistance and those relative to cells monolayer resistance.

Usually a measurement without cells on the Transwell is performed to derive the value of the blank resistance (R_{blank}). Given that the resistances are in series, the expression for the cells monolayer resistance is the following:

$$R_{blank} = R_{bm} + R_{tm} + R_{am}$$

$$TEER = R_{bm} + R_{tm} + R_c + R_{am}$$

thus:

$$R_c = TEER - R_{blank}$$

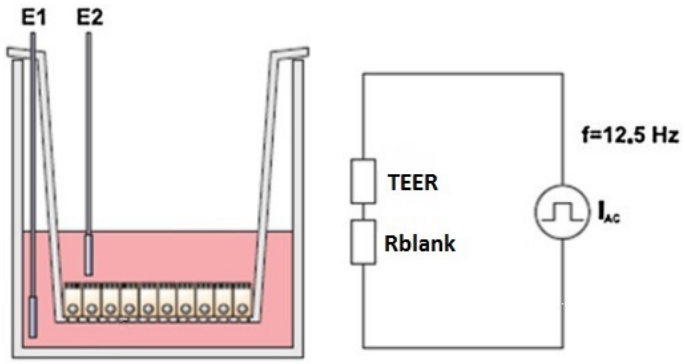

Figure 2.4: Electrical Resistance System

2.2 Reagents

Studies with cultured cells monolayer have been able to identify some signaling pathways for the assembly of the tight junctions. Multiple signal transduction pathways have been implicated in tight junctions biogenesis including Ca^{2+} [11].

EGTA (ethylene glycol tetraacetic acid) is a chelating agent. It has a lower affinity for magnesium, making it more selective for Ca^{2+} ions. It is useful in buffer solutions that resemble the environment in living cells where calcium ions are usually at least a thousandfold less concentrated than magnesium.

When the epithelial cells are treated with EGTA lose the barrier function as the EGTA consumes Ca^{2+} responsible for the formation of tight junctions. When there is low concentrations of Ca^{2+} (μM) the epithelial cells lose apical and basolateral domains and allow a unregulated flux across the monolayer. With low concentrations of Ca^{2+} the TEER is near to zero.

Polyinosinic:polycytidylic acid (usually abbreviated Poly I:C) is an immunostimulant. It is used in the form of its sodium salt to simulate viral infections [12]. The POLY I:C is used to create a viral attack to alter the tight junctions.

2.3 Matlab Simulations

We can simulate the disruption of the barrier with the Equivalent Circuit Model relative to the biochip and we can calculate, with simulations on Matlab, the variations at different frequencies of the biochip impedance. In this way we can know the behavior of the cells' monolayer when the cells are healthy or when they lose the barrier function.

We can use the Equivalent Circuit Model to calculate the values and to simulate the behavior of the cells impedance relative to biochip, at different frequencies and with or without reagents. The Equivalent Circuit Model is simulated with a Matlab Script.

In Matlab Script we have the first part where the parameters values are initialized as the R_{tm}, R_{am}, R_c, C_c, R_m, C_m. The C_c was multiplied for the area relative to electrodes while the C_m was multiplied for the area relative to membrane. The value of TEER is equal at the sum

of R_{blank} (sum between R_{tm}, R_{bm} and R_{tm}) plus R_c so we can obtain for inverse formula the value of R_c. The value of TEER with healthy cells is comprise between 1000Ω and 3000Ω. For this simulation we use the value of TEER 1000Ω.

To simulate the cells stimulated with POLY I:C the TEER value of treated cells measured in a Transwell was used. The same thing was done to simulate the EGTA treatment.

The value of R_c when the cells are healthy is 835Ω while when the cells are treatment with POLY I:C the value of R_c becomes 335Ω and when the cells are treatment with EGTA the value becomes 35Ω.

In Fig. 2.6 and 2.7 are shown the simulations relative to four different conditions

- healthy cells
- cells treated with POLY I:C
- cells treated with EGTA
- no cell layer

When on the biochip there are only the membrane and the medium we have a low impedance compared to when there is the cells' monolayer. When there are healthy cells we have the highest values of the impedance. When the cells are treated with POLY I:C and EGTA the magnitude of the impedance decreases compared to when the cells are healthy because the tight junctions are disrupted. The impedance of the cells is modelled with a capacitor in parallel with a resistor so when the cells' monolayer resistance decrease and when it will be close to zero it will short-circuit the capacitor and so the phase of the biochip will decrease.

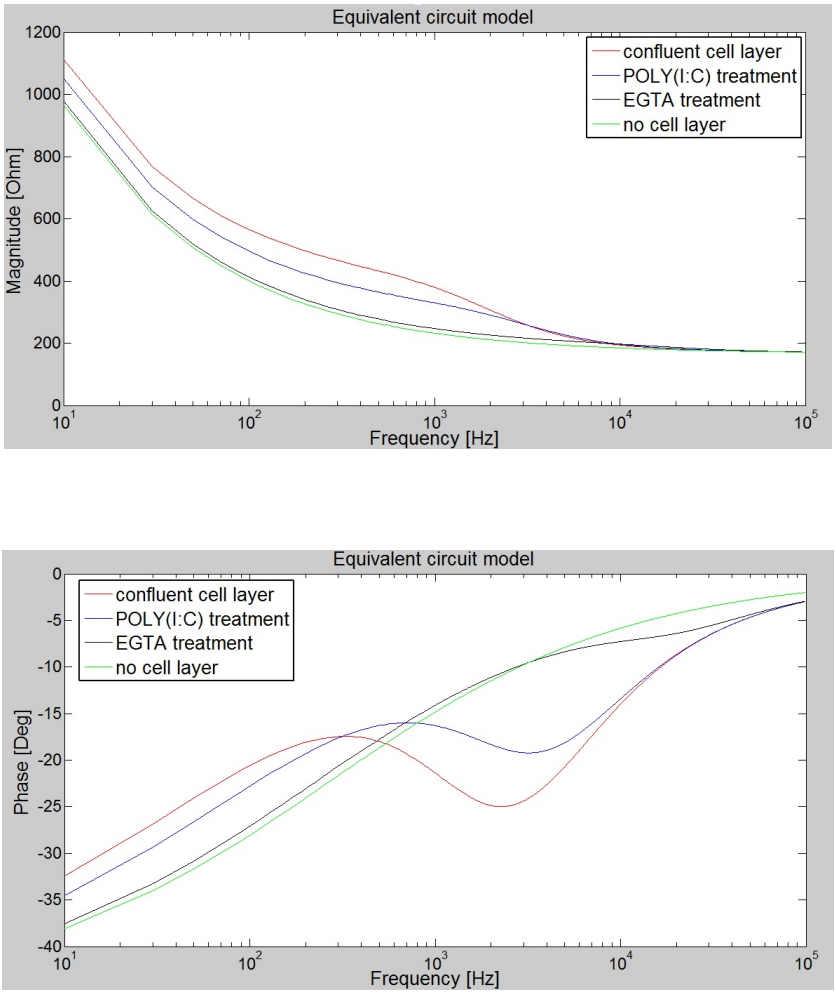

Figure 2.5: Magnitude (top) and Phase (bottom) of the Biochip Impedance by Matlab Simulation

2.3.1 Frequency Input Signal

To have information of the cells impedance we have to apply a potential difference between the electrodes. This stimulus signal is a sinusoidal signal characterized by an amplitude and a frequency. The choice of the frequency of the input signal is based on the amount of signal that we have at any given frequency. We want to choose a frequency where we have the biggest variations between the output signals to permit to the electronic circuit to measure the values of cells' impedance. If we consider the plot relative to behavior of cells' impedance we can see that we have and more signal or more variations between the values of the impedance to 300Hz.

Chapter 3

Biochip Characterization

The value of frequency chosen for the stimulus signal was 300Hz as at this frequency we have the best response of the biochip so at this frequency the problem relative to Double Layer effect arise. The Double layer effect doesn't allow accurate measures at low frequencies. A method for reducing this problem is to increase the surface area of the electrodes through an electrodeposition.

To evaluate the biochip design and also the Equivalent Circuit Model proposed measures of the biochip impedance using an Impedance Analyzer were made. In this way it is possible to check the operation in different conditions and also to check if the electrodeposition decreased the double layer effect.

3.1 Double layer

When a potential difference is applied to electrodes in a electrolytic solution a polarization phenomenon occurs due to electrical double layer effect. This phenomenon doesn't allow an accurate measurement of impedance at low frequencies as it behaves as a capacitor that shields the electric field lines interacting with the cells. To decrease this effect we need to increase the surface area of the electrodes so that the value of the capacitance will increase. In this way at lower frequencies the double layer effect will be of smaller magnitude.

3.1.1 Double layer Model

A double layer is a structure that appears on the surface of an object when it is exposed to a fluid. We consider an aqueous solution rich of ions where a negatively charged electrode is inserted. The electrode will attract the water molecules, the free cations (with the possible cloud of water molecules) and also of the anions adsorbed that they are in a condition of minimum energy. The double layer is described with two layers of charges surrounding the metal solution interface. On the first layer the surface charge is composed with the charges relative to anions adsorbed and on the second layer the surface charge is composed from cations (Fig. 3.1).

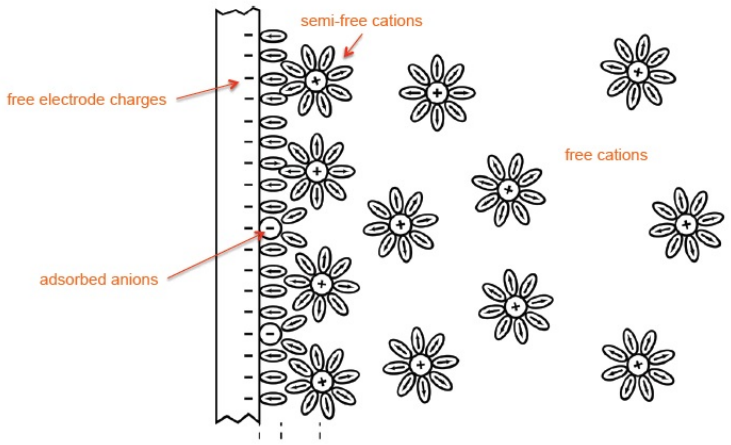

Figure 3.1: General representation of the double layer formed at the metal electrolyte interface [13]

The second layer is composed of ions that move under the influence of electrical attractions and thermal motions, it is called Diffuse Layer.

There are two planes associated with the double layer. The first, inner Helmholtz plane (IHP) passes through the centers of adsorbed ions. The second plane is called outer Helmholtz plane (OHP) and it passes through the centers of the hydrated ions that are in contact with the surface of the metal. The diffuse layer develops outside the OHP.

A curve of potential can plotted as function of the distance from the electrode. On the Stern Layer, close to the electrode, there will be a low dielectric constant relative to water so the molecules are polarized less. The IHP plane is the orders of nm long. In its corrispondence the potential increases as adsorbed ions and solvated molecules cannot polarize. That means the dielectric constant is low . The OHP plane includes dissolved and solvated molecules which have opposite polarity and that make the potential decrease linearly. The potential decreases to the point in which the cations are blocked by the electric field. Whereas in the diffusion layer the potential decreases exponentially as the cations can move freely in the liquid (Fig. 3.2).

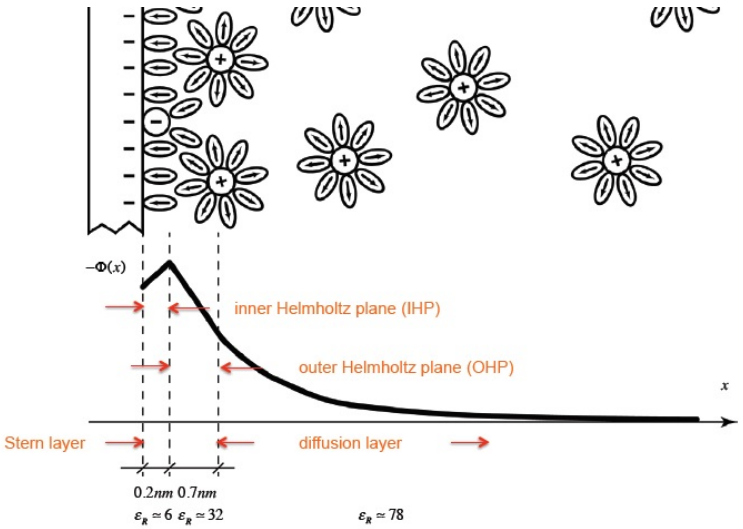

Figure 3.2: Potential profile in the double layer formed at a metallic electrode charged negatively [13]

The parameter that describes the thickness of the electrical double layer is the Debye length. In an electrolytes solution it can be expressed as a function of ionic force of the solution and temperature as:

$$\lambda_D = \sqrt{\frac{\varepsilon_0 \varepsilon_r K_B T}{2 N_A I e^2}}$$

ε_0 : permittivity of free space $\left[\frac{F}{m}\right]$

ε_r : dielectric constant$[-]$

K_B : Boltzmann constant $\left[\frac{J}{K}\right]$

T: absolute temperature $[K]$

N_A : Avogadro number $[mol^{-1}]$

I : ionic strength of the electrolyte $\left[\frac{mol}{m^3}\right]$

e^2 : elementary charge $[C^2]$

A simple model to describe this effect is the Gouy-Chapman-Stern (GCS). In this model at the interface between the electrode and the solution there is a layer of counterions absorbed on the surface: this layer behaves like a parallel place capacitor and will result in a linear potential drop.

The model expected a simplification: the distance from the electrodes is much greater of the Debye Length ($x \gg \lambda_D$). With this simplification the charge density on the Diffuse Layer will be:

$$\sigma_D \approx -\epsilon\alpha\Phi_D$$

σ_D : surface charge $\left[\frac{C}{m^2}\right]$

ϵ : dielectric constant of the solution $\left[\frac{F}{m}\right]$

Φ_D : electric surface potential $[V]$

The feature metal-liquid capacitance can be measured as:

$$C_D = \frac{d\sigma_D}{d\Phi_D} = \epsilon\alpha\cosh(\frac{z_i q}{2kT}\Phi_D) \approx \epsilon\alpha = \frac{\epsilon}{\lambda_D}\left[\frac{F}{m^2}\right]$$

z: valence ionic species

q: electric charge $[C]$

$$\alpha = \frac{1}{\lambda_D}[m^{-1}]$$

k: Boltzmann constant $\left[\frac{J}{K}\right]$

T: Temperature $[K]$

To obtain the data relative capacitance of double layer and Debye length it is necessary to know the ionic concentrations of the solution where the metal is placed. In example for a 1mM KCl:

$$\lambda_D \approx 10nm \rightarrow C_D \approx 70 \cdot 10^{-3}\left[\frac{F}{m^2}\right] = 7.0\left[\frac{\mu F}{cm^2}\right]$$

It is possible to schematic the double layer effect with two capacitors in series. One relative to Stern Layer, calculated as the series of the capacitors of the OHP plane. The other relative to Diffuse Layer (Fig. 3.4)

$$\frac{1}{C_{DL}} = \frac{1}{C_D} + \frac{1}{C_{S1}} + \frac{1}{C_{S2}}$$

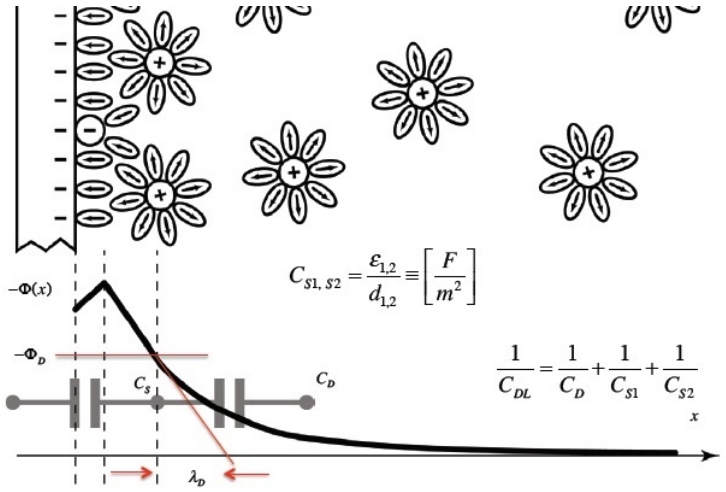

Figure 3.3: Double Layer Capacitance [13]

3.1.2 Electrical Double Layer Effect

The figure 3.4 shown the simulations of Equivalent Circuit Model relative to biochip when the value of the double layer capacitance is almost $2\mu F$. In particular we can see that at low frequencies the capacitor of double layer dominates as we have a high values for the magnitude and phase displacement relative to the biochip simulations. Also we can't calculate the variations of cells impedance for different conditions as the behavior and the values of the impedance are very close and the curves that describe them are overlapping.

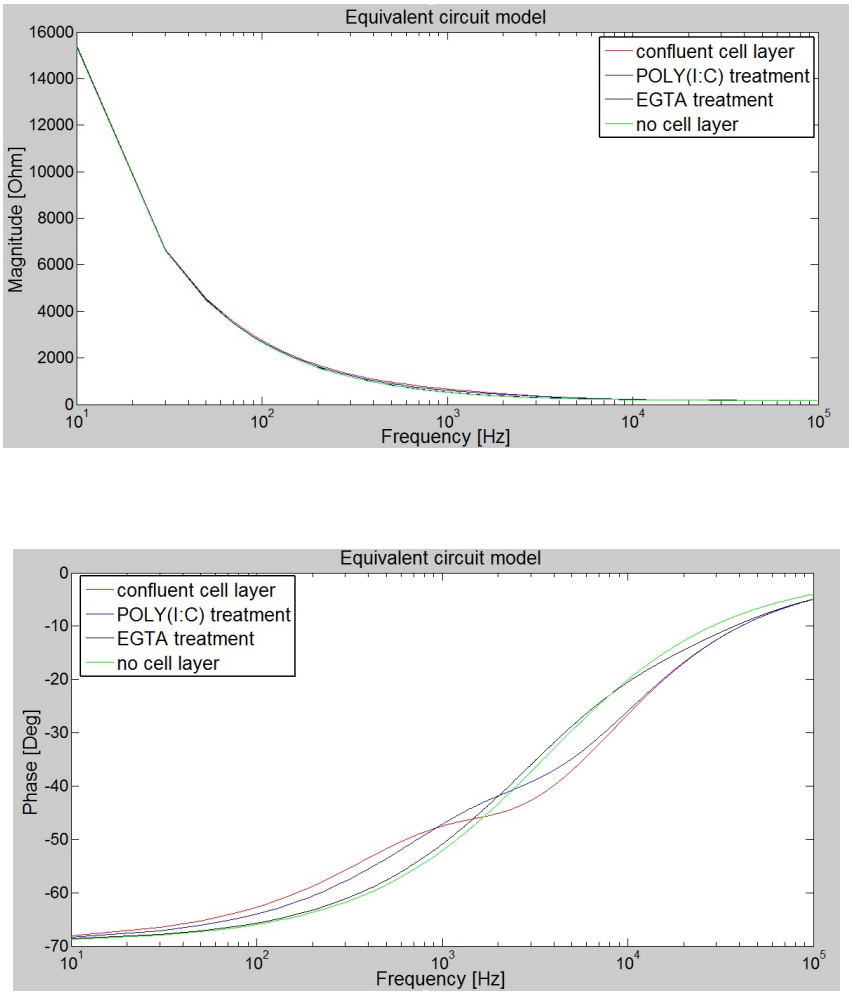

Figure 3.4: Magnitude (Top) and Phase (Bottom) of the biochip impedance with Double Layer Effect

The value of the double layer capacitance has been estimated by fitting the magnitude and phase values of the biochip. The equivalent circuit model describes the biochip when there are no cells. The fitting was made with Zview (Fig. 3.5, 3.6), in particular was assumed that the values of the other components of the model were constant.

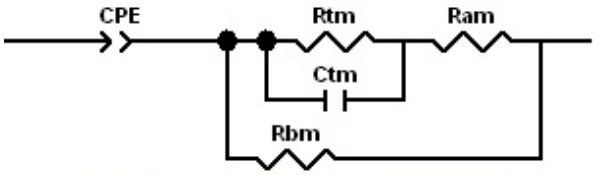

Element	Freedom	Value	Error	Error%
CPE-T	± Free(±)	2.7279E-6	2.3213E-8	0.85095
CPE-P	± Free(±)	0.77036	0.0017188	0.22312
Rtm	X Fixed	48	N/A	N/A
Ctm	X Fixed	4.700E-11	N/A	N/A
Ram	X Fixed	198	N/A	N/A
Rbm	X Fixed	500	N/A	N/A

Figure 3.5: Equivalent Circuit Model of the biochip without cells monolayer

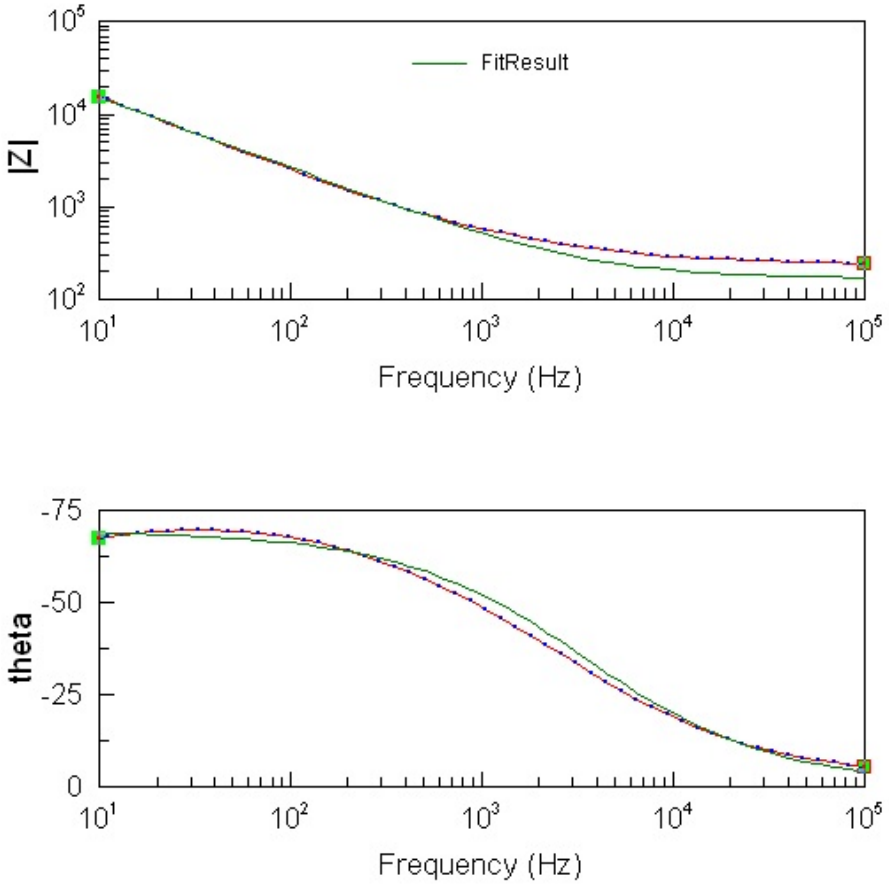

Figure 3.6: Fitting to estimate the value of the double layer capacitance

The electrodes were designed to minimize the double layer effect. This can be done assigning big surface to the electrodes, given that it is:

$$Q = C\Delta V$$

Q: electric charge [C]
C: capacitance [F]
V: potential difference [V]

$$C = \frac{A\varepsilon}{d}$$

A: area electrodes $[m^2]$
ε: permittivity of the dielectric $\left[\frac{F}{m}\right]$
d: thick electrodes [m]

by increasing the surface area the capacity will increase. By increasing the capacitance the potential drop experienced by the system due to a fixed amount of charge will decrease.

To increase the surface area it is possible to deposit porous material (with an high specific area) on top of the electrodes. This is usually done by black platinum deposition on platinum electrodes.

3.1.3 Electrodes Biochip

To measure the output signal there are two pair of electrodes one being dot-ring shaped and the other being straight (Fig.7). The dot and ring are used to measure the impedance of the cells as they are placed below the membrane and the cells, whereas the straight electrodes are used to measure the medium conductivity to account for changes in the temperature. The straight electrodes don't interact with the cells they bring information only relative to the medium conductivity. In this way, it is possible to understand when the impedance changes as there was a change of the cells resistance or as there was a change of medium conductivity.

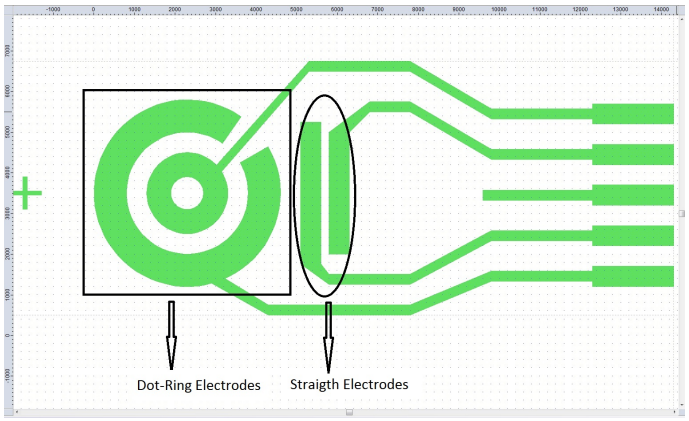

Figure 3.7: Dot Ring and Straight Electrodes

3.1.4 Electrochemical deposition of Pt black

The effect of electrode polarization can be minimized by maximizing the electrode-electrolyte interface area. The most common electrochemical method is the platinum (Pt) black treatment, where platinum is electrodeposited on the surface of a smooth platinum electrode with a high effective area. In Fig. 3.8 shows a typical impedance spectra for each electrode material as Platinum, Iridium Oxide (IrOx), and Polypyrrole/Polystyrenesulfonate (PPy/PSS) and Platinum black. The data shows that the double layer capacitance dominates the behavior of the plain Pt electrodes across the entire measured spectrum; the impedance of the other materials is dominated by resistance down to a few hertz [14, 15].

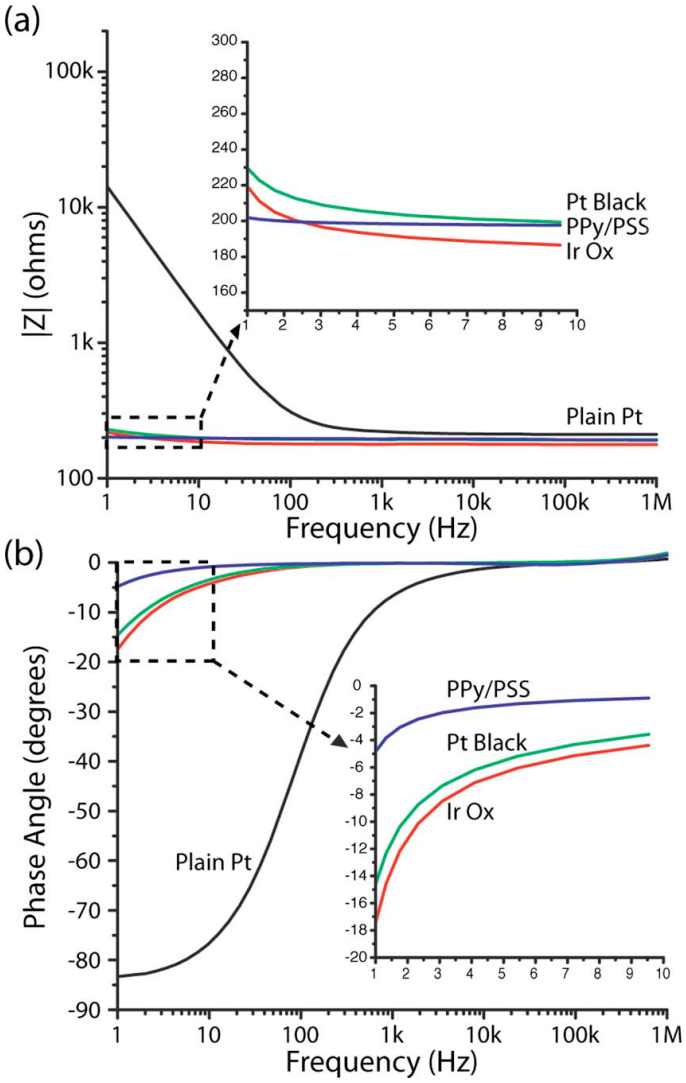

Figure 3.8: Impedance magnitude (a) and phase (b) for bright platinum, Pt black, IrOx and PPy/PSS-coated electrodes [15]

The procedure to perform electroplating is the following: in a beaker, where there is the solution of the metal that has to be deposited, two electrodes are placed. The cathode constitutes the object that you want to cover while the anode can be formed from the metal of the object that you want to cover. A potential difference is applied between the electrodes so that a current will generate.

In this conditions, the cations of the metal that you want to cover move toward the cathode (negatively charged) while the anions move toward the anode (positively charged). In this way we have the purchase of electrons to the cathode (reduction) and and production of electrons at the anode (oxidation).

On the cathode will settle the cations, which gain electrons to the anode and turn into metal atoms. In this way, the cathode is slowly coated with a thin metal layer and the anode is slowly consumed releasing ions in solution.

The set-up for the deposition (Fig. 3.9) of Pt was a power supply where we can set the voltage and the max current to be applied at the solution. A support to hold the electrodes and dip them into the solution was built. We have to use a working electrode and a counter electrode. A beaker was used to contain the platinizing solution and the electrodes. The platinizing solution consisted of 3.5% chloroplatenic acid and 0.005% lead acetate. The working electrode was immersed into the platenizing solution in order to electrochemically deposit high surface area platinum black. Against a Pt counter electrode, a constant potential of 3.5V was applied for 190 seconds [16].

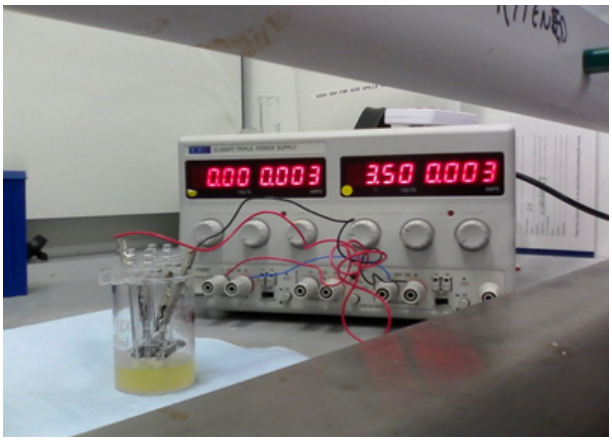

Figure 3.9: Set-up for the Electrochemical deposition of Pt

3.1.5 Impedance response of Pt black coated electrodes

Several checks (as viewing under the microscope after the deposition the coated electrodes, measuring the increment of high surface with a Profilometer and at the end the measuring of the biochip impedance with a Impedance Analyzer) were made to tweak the deposition parameters.

After the deposition we can see of the coated electrodes under the microscope (Fig 3.10). In particular we can see the uniformity of the deposition of each electrodes and the different colour between the dot e ring electrodes and the straight electrodes as these have different areas: the current density depends on the surface area so in the same time on the electrodes largest we have less deposition and a colour lighter.

In addition to the inspection of the electrodes under the microscope, a measurement of the increased height of the surfaces of the electrodes was performed with a Profilometer to validate the deposition procedure. The height is increased by $38\mu m$.

Figure 3.10: Image Coated Electrodes (Top) and Images Coated Electrodes under the microscope (Bottom)

The value of the double layer capacitance has been estimated by fitting of the magnitude and phase values of the biochip impedance with coated electrodes, extracted from measurements made with an Impedance Analyzer. The fitting has made with Zview (Fig. 3.11, 3.12), also in this case was supposed that the values of the other components of the model were constant. The value of the double layer capacitance when the electrodes are coated is almost $150\mu F$

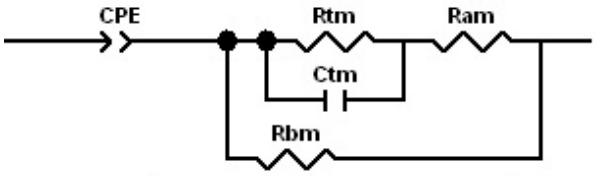

Element	Freedom	Value	Error	Error%
CPE-T	± Free(±)	0.00015969	6.77E-6	4.2395
CPE-P	± Free(±)	0.51048	0.0079978	1.5667
Rtm	X Fixed	48	N/A	N/A
Ctm	X Fixed	4.700E-11	N/A	N/A
Ram	X Fixed	198	N/A	N/A
Rbm	X Fixed	500	N/A	N/A

Figure 3.11: Equivalent Circuit Model of the biochip without cells monolayer with coated electrodes

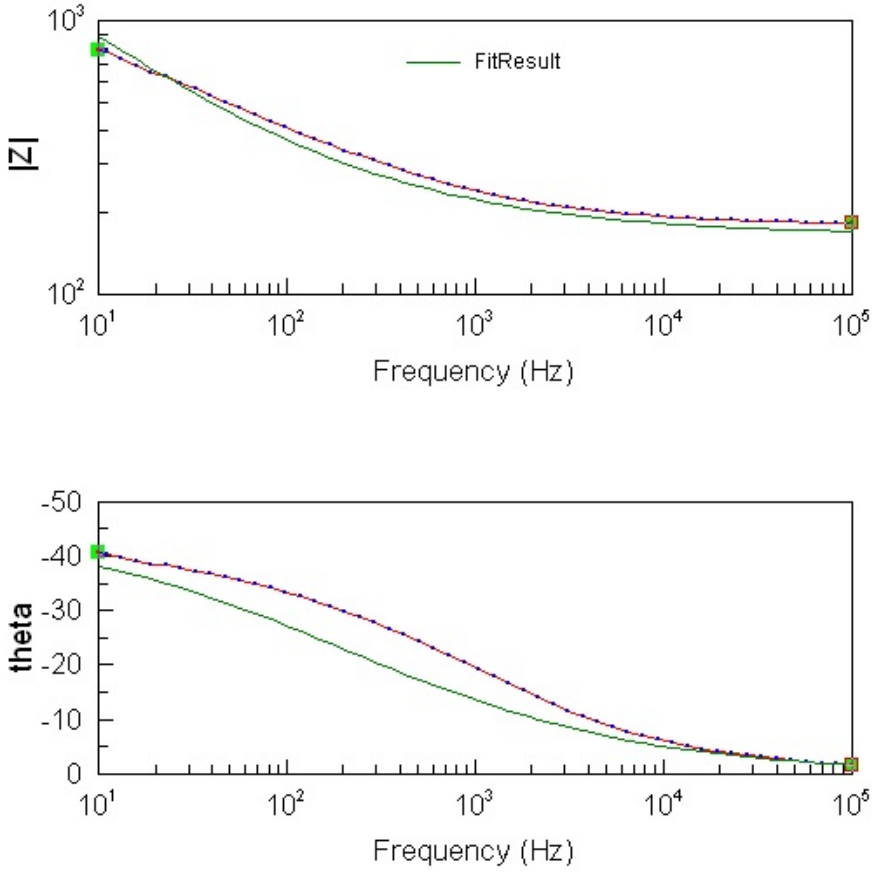

Figure 3.12: Fitting to estimate the value of the double layer capacitance when the electrodes are coated

3.2 Spectroscopy of Impedance

Electrochemical impedance spectroscopy (EIS) is a technique frequently used in microscopic analysis and solid-state investigation. This technique measure the impedance of the electrochemical cell over a range of frequencies, giving information on dissipative and energy storing phenomenon [17]. EIS can give a global characterization relative to linear dynamic system from study of the transfer function.

The electrical impedance is defined as the ratio of an incremental change in voltage to the resulting change in current (or vice versa) across the electrochemical system. When a sinusoidal voltage signal is applied:

$$V_{REF}(t) =\mid V_{REF} \mid \sin(\omega_0 t)$$

across the system and assuming linear behavior, we expect the corresponding current to be:

$$I(t) =\mid I \mid \sin(\omega_0 t + \theta)$$

where θ is the phase shift of the signal with respect to the excitation. The relation between the excitation and the measured signal is the impedance Z. The impedance can defined using the phasors as:

$$Z(j\omega) = Re(Z) + jIm(Z) =\mid Z \mid e^{-j\theta}$$

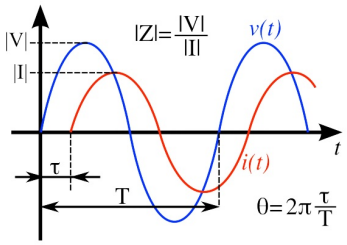

Figure 3.13: Typical applied voltage to electrochemical cell (blue line) and related flowing current (red line)

3.2.1 Alpha-A Analyzer Novocontrol

This system features high performance dielectric, conductivity, electrochemical, impedance and gain phase measurements in the frequency domain. The system is modular and based on an Alpha-A mainframe unit which usually is combined with one or more test interfaces optimized for special functionality. All test interfaces for impedance measurement offer in addition high general purpose performance like highest accuracy and ultra wide impedance and frequency range. This makes the Alpha-A system an unique and easy to use instrument with exceptional overall performance which suits in addition many special requirements like e.g. 4 electrode high impedance, high voltage, high current measurements and potentiostat, galvanostat functions for electrochemical impedance spectroscopy EIS.

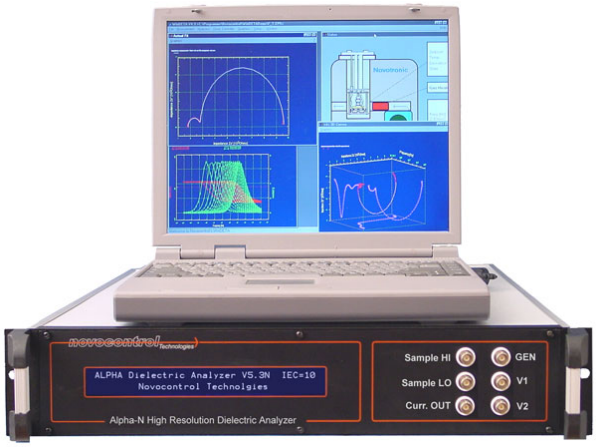

Figure 3.14: Novocontrol Alpha-n high resolution dielectric analyzer

3.2.2 Biochip impedance to Check the Electrical Double Layer Effect

To check if the deposition of Pt black decreased the electrical double layer effect we have to measure the impedance of the biochip with an Impedance Analyzer (Novocontrol) and in particular we have to compare the results between a biochip with coated electrodes and a biochip with uncoated electrodes. To do so the electrodes are connected to the Impedance Analyzer where we can set the range of frequency, the number of points to sample. To establish the flow conditions the biochip is connected to a syringe pump. The flow rate was set to 30 ml/hr.

In the figure 3.15 we can see the magnitude and phase of the biochip impedance with coated and uncoated electrodes. When we measure the uncoated we can see that a low frequency dominates the capacitance of double layer. When we measure the coated electrodes we can see that at low frequency the effect of the double layer decreases as the values of magnitude are decreased and that there is less phase displacement.

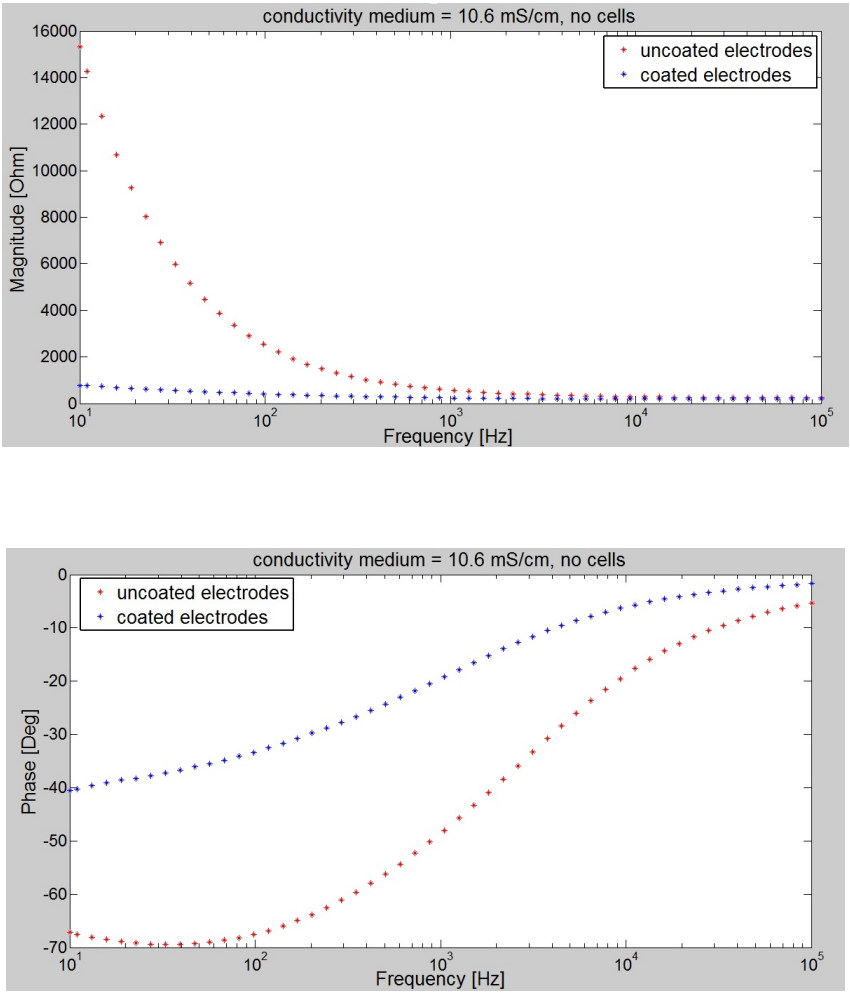

Figure 3.15: Magnitude (Top) and Phase (Bottom) of the biochip impedance with coated electrodes and uncoated electrodes

3.3 Impedance Measurement with Novocontrol

The characterization of the system consists in making impedance measurements of the biochip with an Impedance Analyzer in different configurations to verify the design of the biochip and to validate the simulations made with matlab. In particular we want to obtain the same trends of the impedance when in biochip is pumped with medium with different conductivity values, differents flow rates and with or without the presence of the apical medium.

3.3.1 Experimental Measurement of the Biochip Impedance

The set-up to do this measurements was: a syringe pump where we can set the flow rate of medium, a biochip positioned in a support where we can connect the electrodes with the Novocontrol by two crock-clip. The inlet of the biochip is connected with the syringe pump and the outlet is placed above a beaker. On the Novocontrol were set the range of the frequency, the number of points to sample. The measured range of frequency was from 100Hz to 10KHz.

To characterize the system and to validate the Matlab simulations measures with a medium with conductivity of $3.95\frac{mS}{cm}$, $2020\frac{\mu S}{cm}$, $520\frac{\mu S}{cm}$ were done. For each conductivity measurements of the biochip impedance on straight electrodes and dot and ring electrodes were done, with apical or without and with different flow rates for the medium.

When the conductivity increase we can see that the impedance decrease as the impedance depends on conductivity with the expression $R = \frac{K}{\sigma}$ where K is the cell constant. This value depends on the geometric factors of the electrodes. When we have the apical medium, the biochip impedance increases as we add a resistor in parallel our system. When we change the flow rate we have a neglectable change of the impedance as it doesn't depend from the flow rate.

The figures 3.16, 3.17, 3.18 show the magnitude of the impedance with different conductivities and different flow rates for the medium. In particular we can see that the values of magnitude increase when the conductivity decrease from theory. The same figures show the phase of the impedance and we can see that the values change for differents conductivity of the medium as the double layer capacitance depends of values of the concentration of the solution in which the electrodes are immersed. At high frequencies the values of the phase for different conductivities of the medium are almost the same as the effect of the capacitors tends to zero.

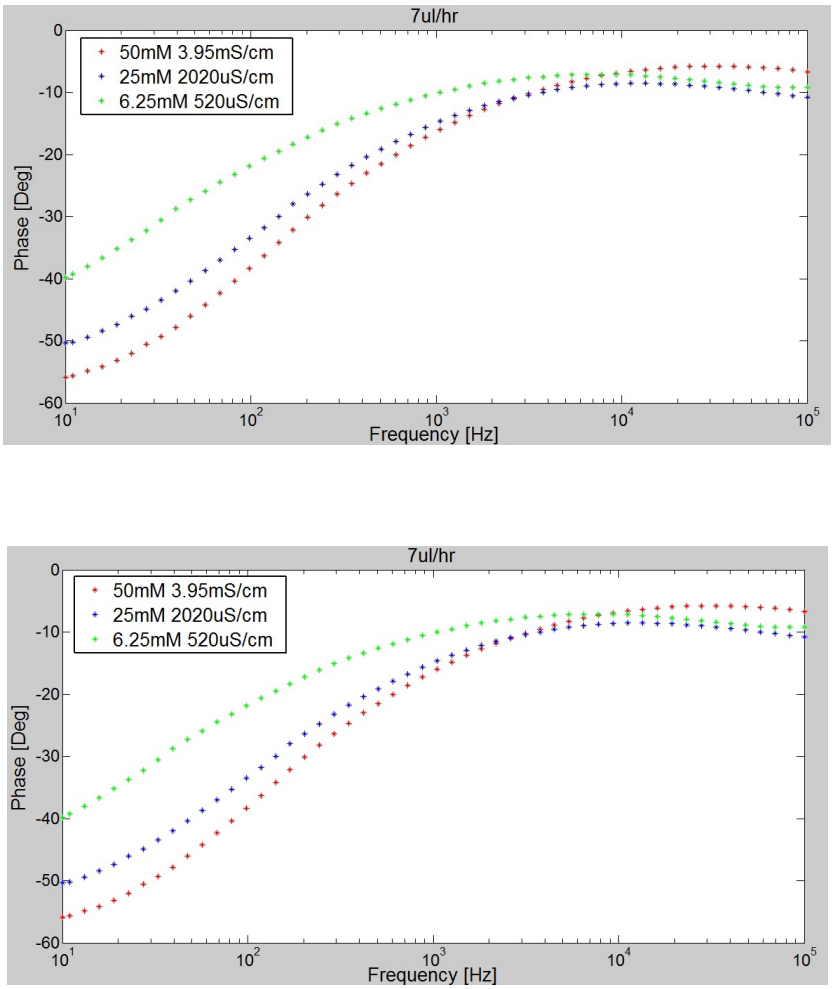

Figure 3.16: Magnitude (Top) and Phase (Bottom) of the Biochip Impedance without cells , for the Dot and Ring electrodes, with Double Layer Effect and medium flow rate of 7ul/hr

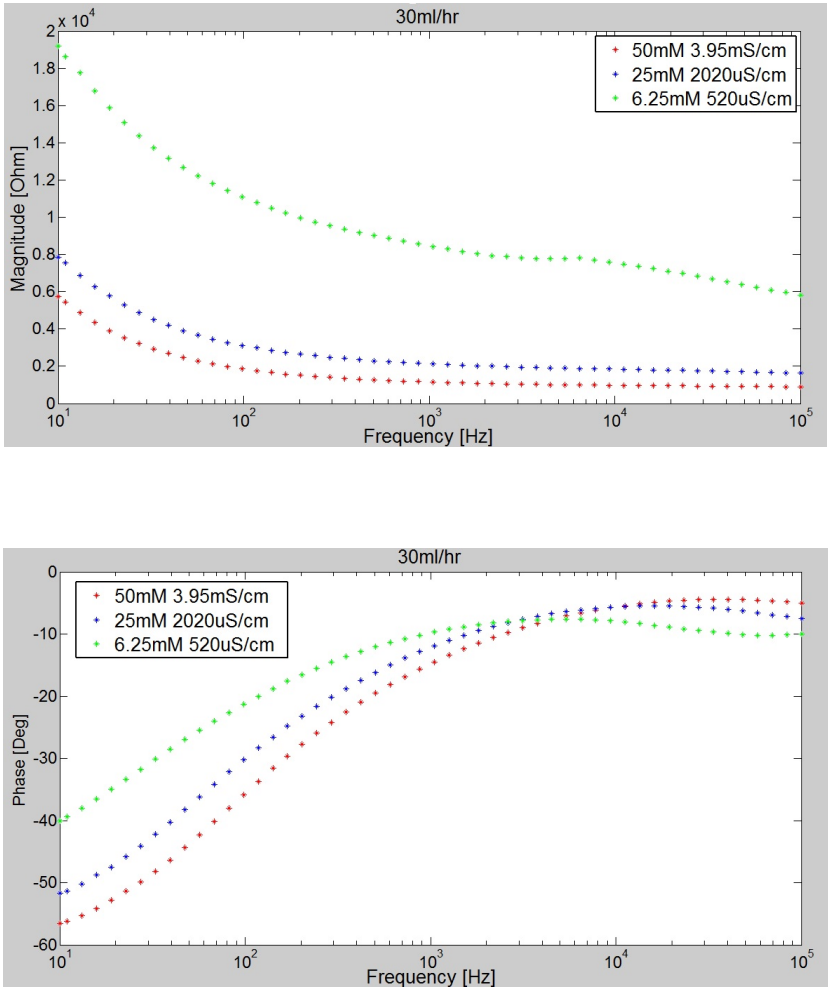

Figure 3.17: Magnitude (Top) and Phase (Bottom) of the Biochip Impedance without cells, for the Dot and Ring electrodes, with Double Layer Effect and medium flow rate of 30ml/hr

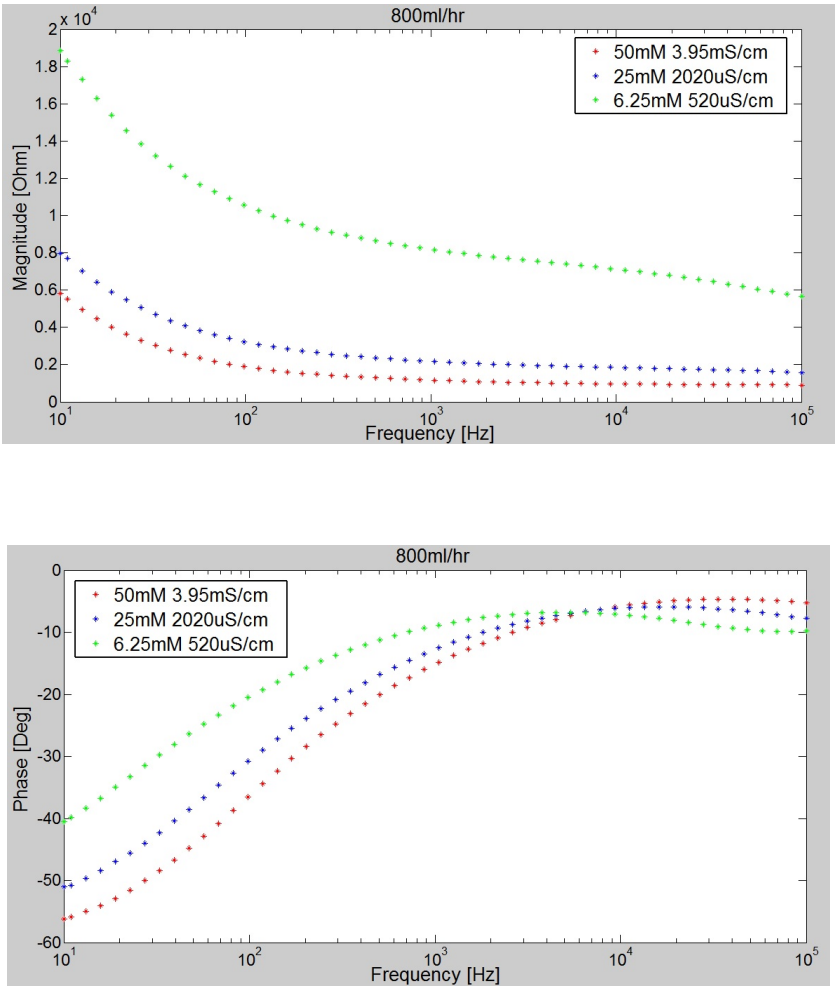

Figure 3.18: Magnitude (Top) and Phase (Bottom) of the Biochip Impedance without cells, for the Dot and Ring electrodes, with Double Layer Effect and medium flow rate of 800ml/hr

The figure 3.19 shows measurements with different flow rates and a medium concentration of 50mM and we can see that the values of magnitude and phase of the impedance don't depend on the flow rate.

The figure 3.20 shows that the values of magnitude increase when we add apical medium to the biochip because we add a resistor in parallel to another resistor and this confirms that the Equivalent Circuit Model described earlier characterizes the operation of the biochip.

The figure 3.21 shows the values of magnitude when the input signal is applied between the straight electrodes. The values of the magnitude of the impedance are higher compared to those of the dot and ring electrodes. Because the cell constant is bigger for the former. The straight electrodes have a surface smaller compared to the dot-ring electrodes. We have a bigger capacitance with a smaller surface. In the equivalent model the double layer capacitance is in series. This explains the greater effects on the phase when the measurements are done using straight electrodes.

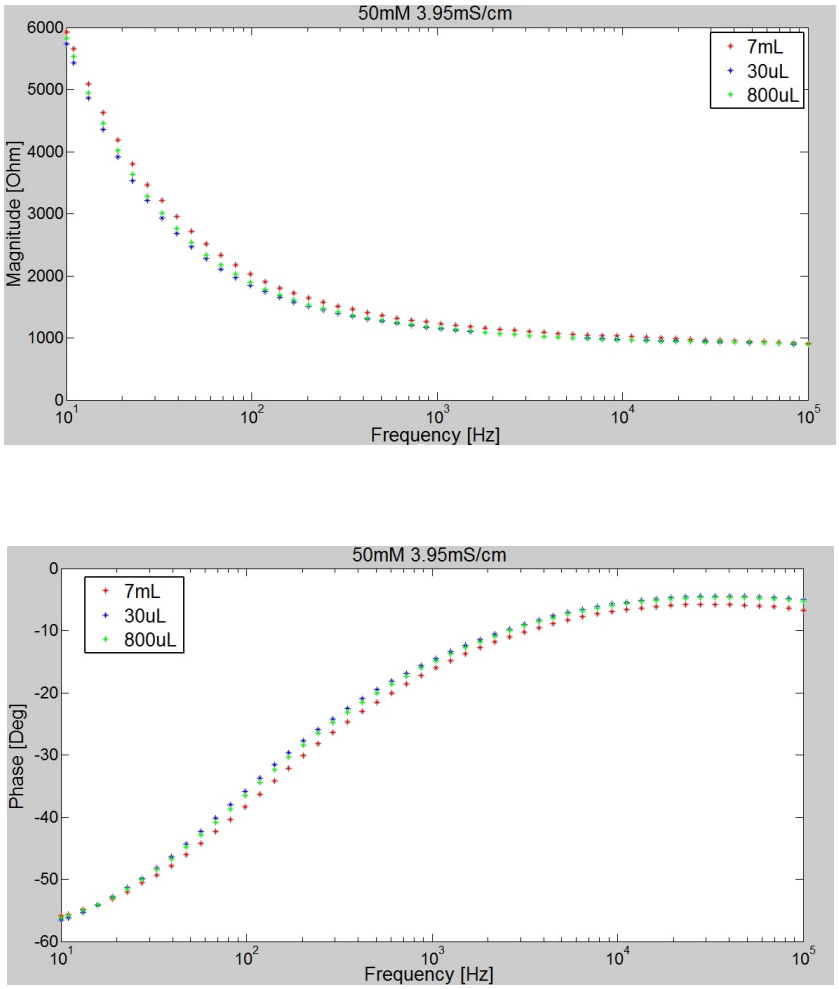

Figure 3.19: Magnitude (Top) and Phase (Bottom) of the Biochip Impedance without cells, for the Dot and Ring electrodes, with Double Layer Effect and medium conductivity of 30mS/cm

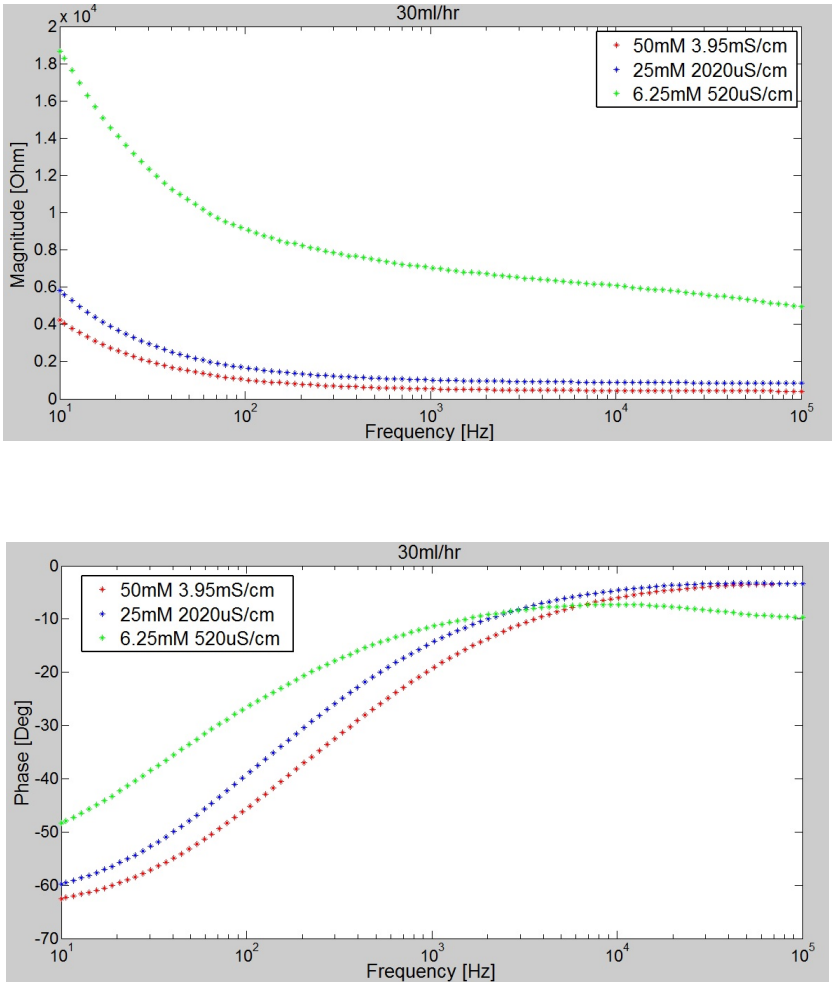

Figure 3.20: Magnitude (Top) and Phase (Bottom) of Biochip Impedance without cells, for the Dot and Ring electrodes, with Apical, with Double Layer Effect and medium flow rate of 30ml/hr

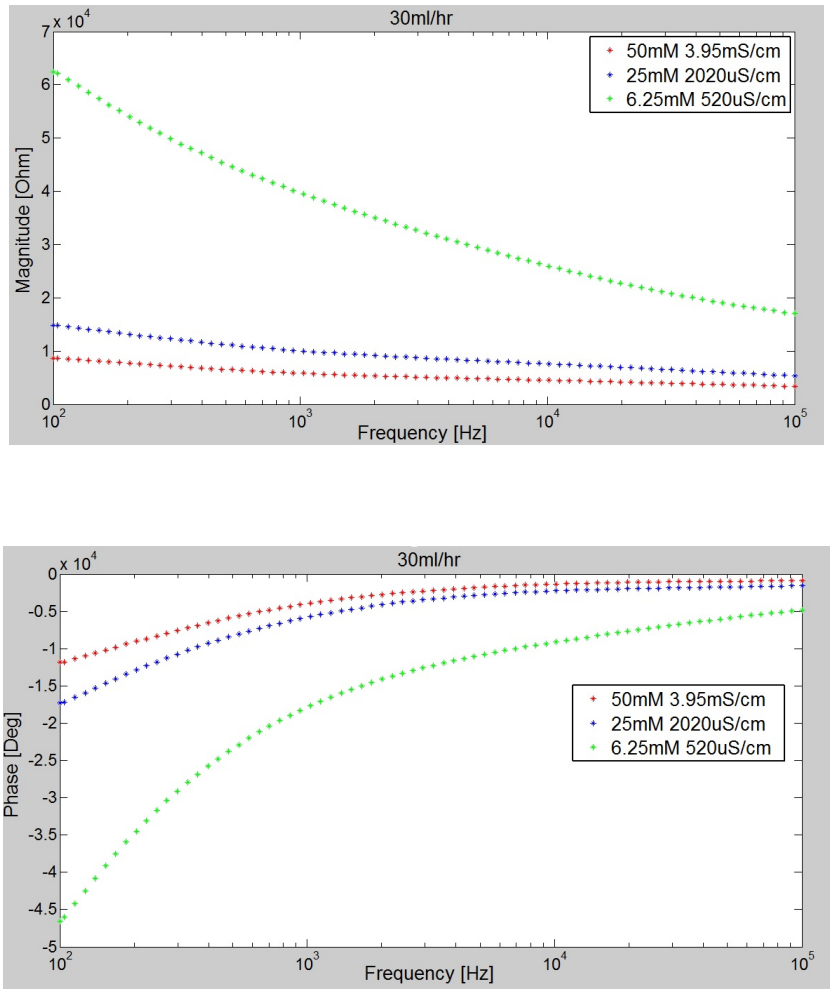

Figure 3.21: Magnitude (Top) and Phase (Bottom) of the Biochip Impedance without cells, for the Straigth Electrodes, with Double Layer Effect, medium flow rate of 30ml/hr

The Fig. 3.22, 3.23, 3.24 show the same measurements with coated electrodes. When the results are compared we can see that the effects of double layer decreases given that the values of the magnitude of the impedance for coated electrodes at low frequencies are lower and there are less capacitive effects affecting the phase.

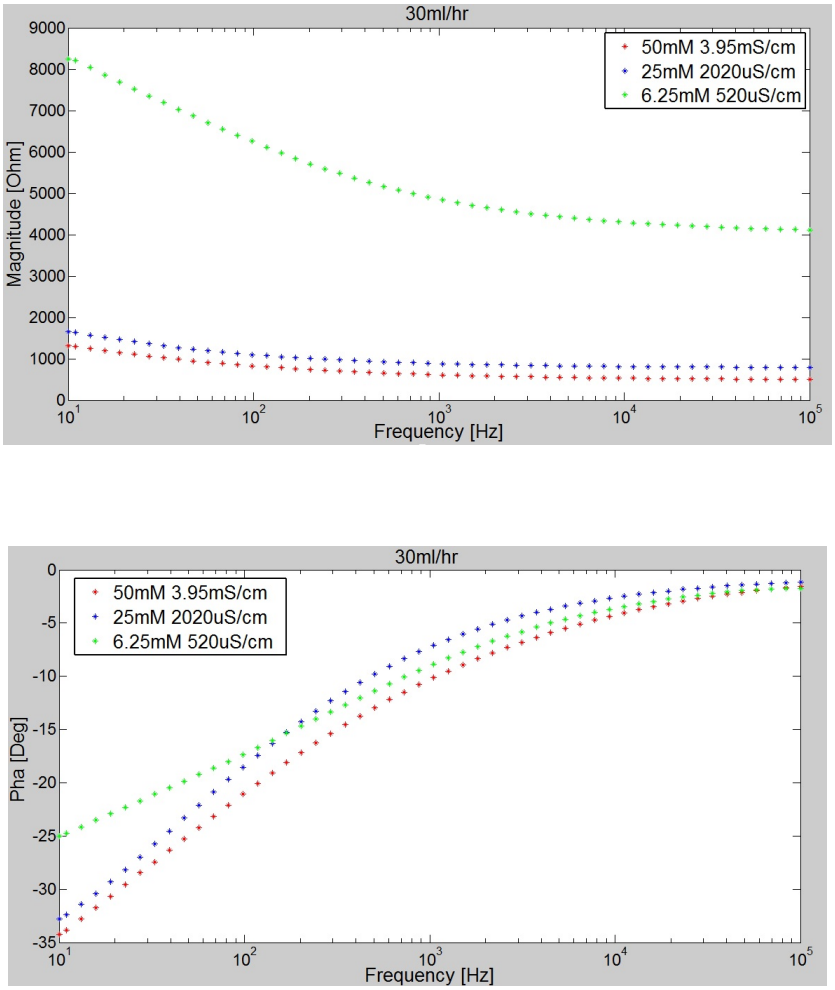

Figure 3.22: Magnitude (Top) and Phase (Bottom) of the Biochip Impedance without cells, for the Dot and Ring Electrodes, no Double Layer Effect and medium flow rate of 30ml/hr

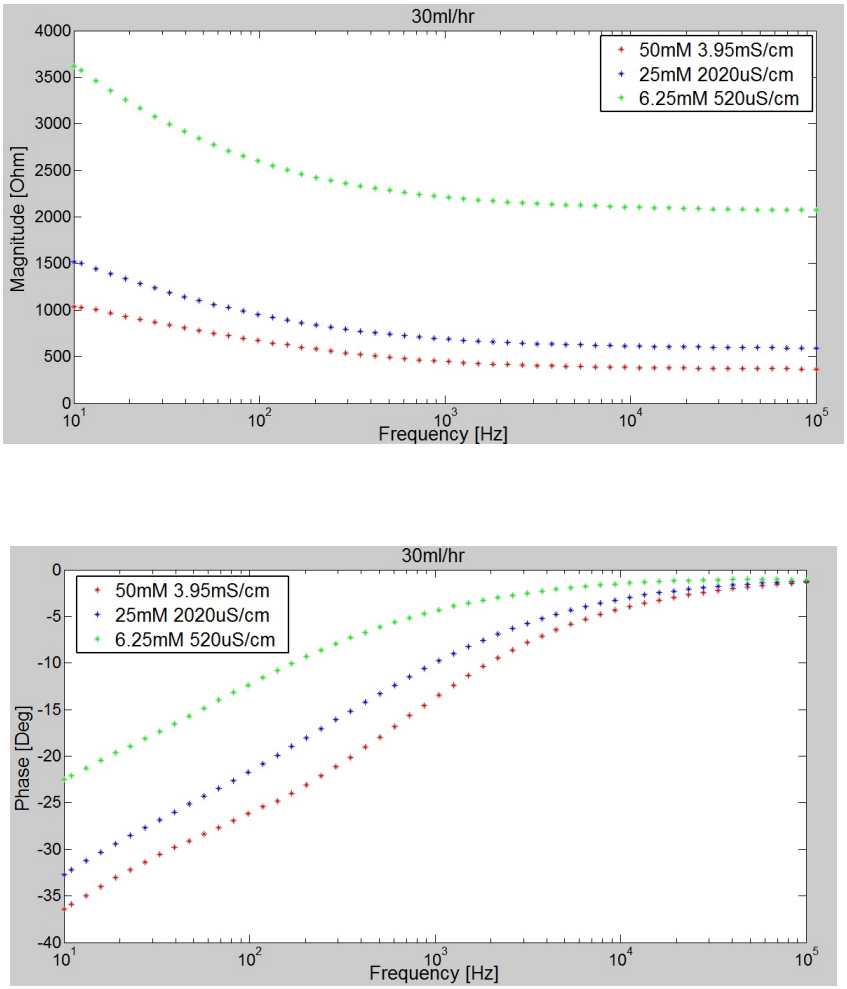

Figure 3.23: Magnitude (Top) and Phase (Bottom) of the Biochip Impedance without cells, for the Dot and Ring Electrodes, with Apical, no Double layer Effect and medium flow rate of 30ml/hr

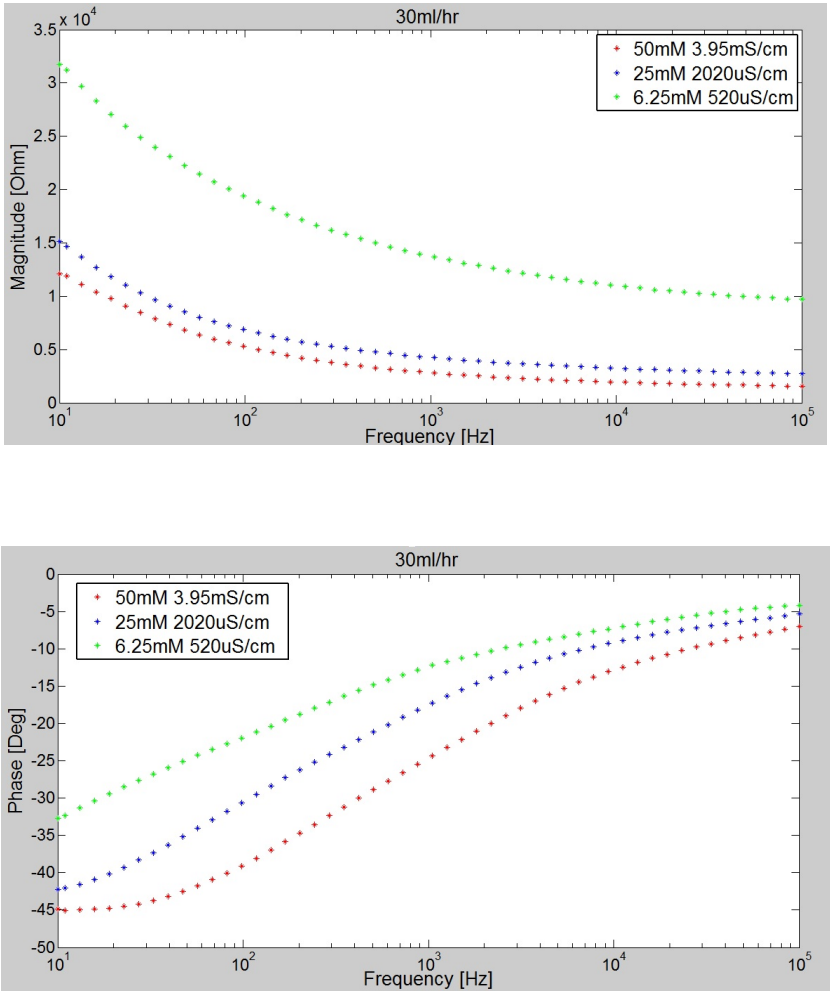

Figure 3.24: Magnitude (Top) and Phase (Bottom) of the Biochip Impedance without cells, for the Straigth Electrodes, no Double Layer Effect and medium flow rate of 30ml/hr

To check the relationship between the magnitude of the impedance and the medium conductivity, the magnitude was measured for six different values of the medium conductivity with a frequency spectrum between 10 Hz and $10^5 Hz$. The set-up used is the same as that used for the characterization tests and evaluation of the double layer effect. Then, at the frequency the values of the conductivity were plotted against the magnitude of the biochip impedance. The measured data follow the theoretical hyperbolic relation $R = \frac{K}{\sigma}$.

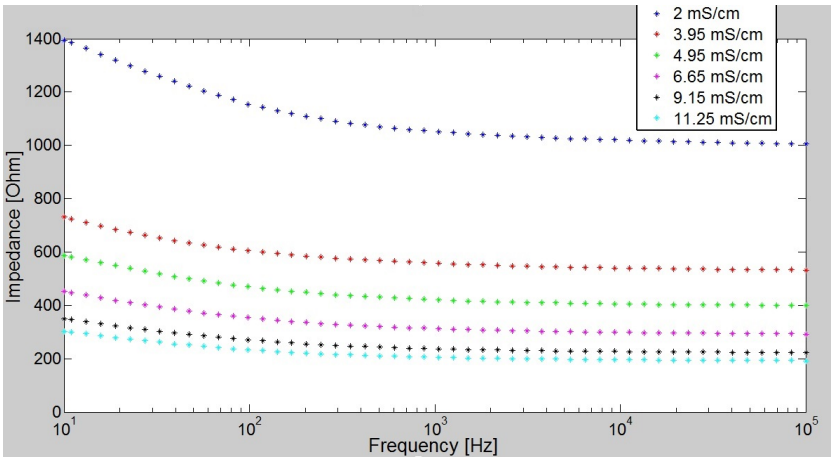

Figure 3.25: Magnitude of the Biochip Impedance without cells, for the Dot and Ring electrodes, no Double Layer Effect and medium flow rate of 30ul/hr

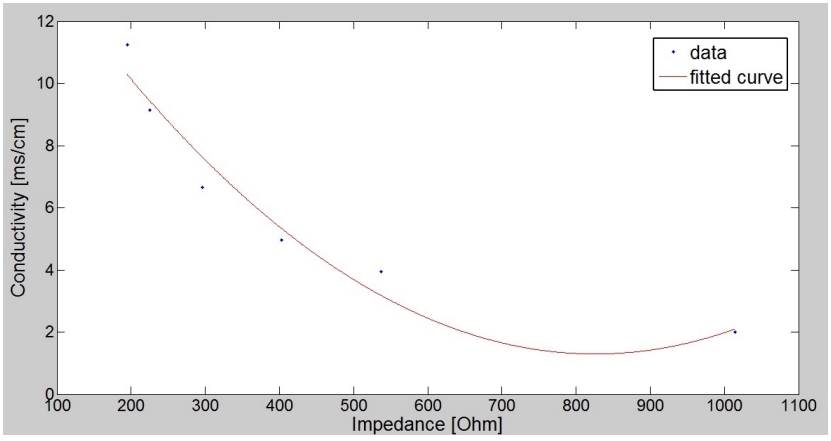

Figure 3.26: Relation between Magnitude of the biochip impedance and conductivity of the medium. Fitting DATA, R-Squared = 0.95

Chapter 4

System Instrumentation

The circuit that we will use to measure the signal output from the biochip is a lock-in amplifier. A lock-in amplifier can measure small AC signal of nanoVolts even in the presence of noise sources of much greater amplitude. The design of the PCB has to allow a measure of the impedance and it should be low-cost and portable [18]. The working principle of the PCB design will be based on the idea of complex impedance by Lock-in amplifier. With this circuit we can measure the biochip impedance and study the behavior of epithelial cells monolayer.

4.1 Lock-in Amplifier

Lock-in amplifiers use a technique known as phase-sensitive detection to single out the component of the signal at a specific reference frequency and phase. Noise signals, at frequencies other than the reference frequency, are rejected and do not affect the measurement.

An example for the use of Lock-in can be given as follows: Suppose the signal is a 10nV sine wave at 10KHz definitely some amplification is required to bring the signal above the noise. A good low-noise amplifier will have $5\frac{nV}{\sqrt{Hz}}$ of input noise. If the amplifier bandwidth is 100KHz and the gain is 1000, we can expect that the output will be $10\mu V$ of signal ($10nV \times 1000$) and 1.6mV of broadband noise ($5\frac{nV}{\sqrt{Hz}} \times \sqrt{100}KHz \times 1000$). The noise signal is bigger that the useful signal,

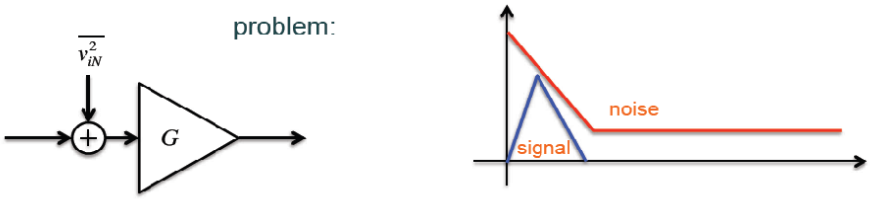

Figure 4.1: Lock-in principle [19]

this means that the measurement of the signal is not possible.

Now we can try the amplifier with a phase-sensitive detector (PSD). The PSD can detect the signal at 10KHz with a bandwidth as narrow as 0.01Hz! In this case, the noise in the detection bandwidth will be 0.5 μV ($5\frac{nV}{\sqrt{Hz}} \times \sqrt{0.01Hz} \times 1000$), while the signal is still $10\mu V$. The signal-to-noise ratio is now 20, and an accurate measurement of the signal is possible.

4.1.1 Phase-Sensitive Detection

Typically, a device is excited at a fixed frequency (from an oscillator or function generator), and the lock-in detects the response from the device. This system requires to modulate the input signal before that it is affected from the noise with a sinusoidal signal:

$$V_R(t) = V_R \sin(\omega_0 t + \theta_R)$$

After the modulation, the signal is affected from the noise and it will be amplified and demodulated using a multiplication by another sinusoidal signal:

$$V_L(t) = V_L \sin(\omega_0 t + \theta_L)$$

The output will be the same that we would have with no modulation/demodulation but with a much lower noise as its peak will end at high frequencies.

The signal after the amplification is:

$$V_B(t) = x(t)GV_R \sin(\omega_0 t + \theta_R)$$

where $x(t)GV_R$ is the signal amplitude, ω_0 is the signal frequency, and θ_R is the phase of the signal.

The lock-in amplifies the signal and then multiplies it by the lock-in reference using a phase-sensitive detector or multiplier. The output of the PSD is simply the product of two sine waves:

$$V_P(t) = x(t)GV_R V_L \sin(\omega_0 t + \theta_r) \sin(\omega_0 t + \theta_l) =$$

$$= \frac{1}{2} x(t)GV_R V_L [\cos(\omega_R - \omega_L) - \cos(2\omega_0 t + \theta_R + \theta_L)]$$

If the PSD output is passed through a low pass filter, the AC signals are removed as shown in figure 4.2.

If ω_R equals ω_L, the difference frequency component will be a DC signal. In this case, the filtered PSD output will be:

$$V_O(t) = \frac{1}{2} x(t)GV_R V_L \cos(\theta_R - \theta_L)$$

The signal output will be a DC signal proportional to the signal amplitude.

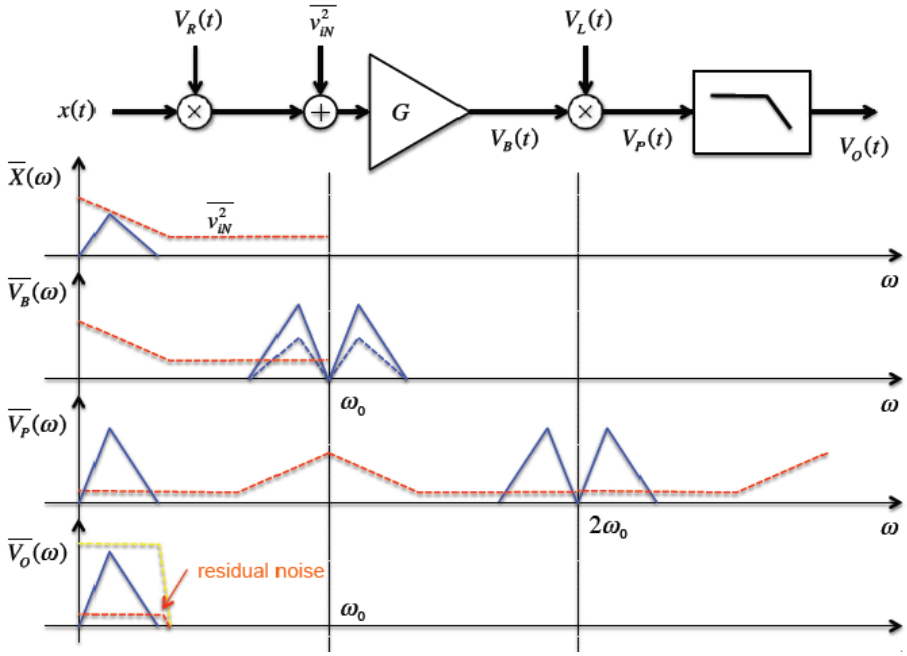

Figure 4.2: Lock-in principle in frequency domain [19]

4.1.2 Narrow Band Detection

The PSD and the low pass filter allow to measure the signal near to the reference frequency. The noise signal at frequencies far away from those of reference is attenuated by low pass filter. Noise at frequencies close to the reference frequency will result in very low frequency AC outputs from the PSD. The attenuation of this noise depends on the bandwidth of the filter. With a smaller bandwidth also this noise will be attenuated so that we can get a true DC output signal.

To get a DC output we have to ensure that the frequency of the signal is equal to the reference frequency so that the phase between the signals can not change with time.

4.1.3 Magnitude and Phase

The PSD output is proportional to:

$$x(t)GV_RV_L\cos\theta$$

where:

$$\theta = (\theta_R - \theta_L)$$

θ is the phase difference between the signal and the lock-in reference. By adjusting θ_R we can make θ equal to zero. In which case we can measure:

$$x(t)GV_RV_L(\cos\theta = 1)$$

Instead, if θ is 90° , there will be no output. A lock-in with a single PSD is called a single-phase lock-in and its output is:

$$x(t)GV_RV_L\cos\theta$$

This phase can be eliminated by adding a second PSD. If the second PSD multiplies the signal with the reference oscillator shifted by 90°, i.e.

$$V_L' = V_L\sin\left(\omega_0 t + \theta_L + \frac{\pi}{2}\right)$$

its low pass filtered output will be:

$$V_O'(t) = \frac{1}{2}x(t)GV_RV_L\sin(\theta_R - \theta_L)$$

Now we have two outputs: one proportional to $\cos\theta$ and the other proportional to $\sin\theta$. We can call
the first output X and the second Y,

$$X = x(t)GV_RV_L\cos\theta$$

$$Y = x(t)GV_RV_L\sin\theta$$

these two quantities represent the signal as a vector relative to the lock-in reference. X is called the "in-phase" component and Y the "quadrature" component. This is because when θ=0, X measures the signal while Y is zero.

We can calculate the magnitude (R) of the signal vector as:

$$R = (X + Y)^{\frac{1}{2}}$$

In addition, the phase (θ) between the signal and lock-in is defined as:

$$\theta = \tan^{-1}\left(\frac{Y}{X}\right)$$

4.2 Complex Impedance Detection by Lock-in

To measure the biochip impedance a lock-in amplifier was used. The working principle is the following: The input signal is a cosine wave with A and ω respectively its amplitude and pulsation. This signal goes in input to the biochip and it creates a potential difference between the electrodes. The potential difference generates a current which depends on the cells impedance. The shape of the current signal is the same as input signal but it will be a different phase displacement due to the impedance of the biochip. We have phase displacement as the biochip impedance is complex. The current signal from the biochip is converted into a voltage signal and amplified. Then the signal is modulated by a signal reference. To do the quadrature detection also the input signal has to have modulated with a signal reference but in this case with a phase displacement of $\frac{\pi}{2}$. The two signals in input from the multipliers go in input a two low pass filter. With the signals in output from the low pass filter is it possible to obtain modulus and phase relative to the biochip impedance as we obtain the real part and the complex of the impedance. The working principle is shown in figure 4.3

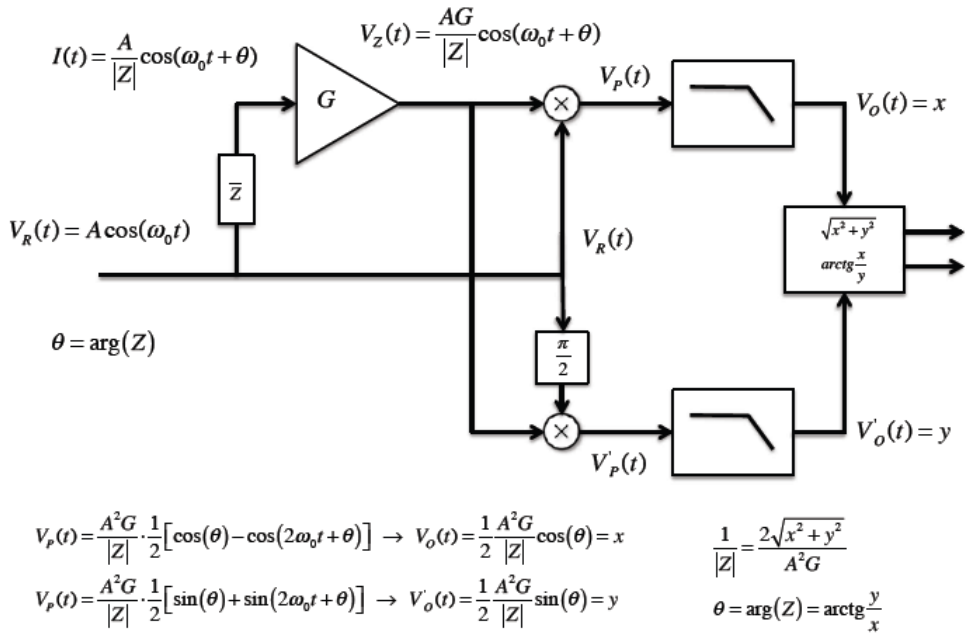

Figure 4.3: Complex impedance detection by Lock-in amplifier [19]

4.3 Noise Sources

There are two types of noise that we have to worry about in laboratory situations: intrinsic noise and external noise. Intrinsic noise sources, like Johnson noise and shot noise, are inherent to all physical processes. we can only minimize the effects of these noises. External noise sources are found in the environment such as power line noise and broadcast stations. The effect of these noises sources can be minimized by careful attention to grounding, shielding, and other aspects of experimental design.

4.3.1 Johnson Noise

Ever resistor generates a noise due to thermal fluctuations in the electron density inside the resistor itself [20]. These fluctuations cause a power of noise:

$$V_{noise}(rms) = (4kTR\Delta f)^{\frac{1}{2}}$$

k: Boltzmann's constant ($1.38 \times 10^{-23} J/K$)
T: temperature in [K] (typically 300 K)
R: resistance [Ω]
Δf :bandwidth of the measurement [Hz]

4.3.2 Shot Noise

The Shot Noise or Current Noise arises from the fact that the current isn't continuous but quantized (it is characterized by small elements but not infinitesimal, the electrons). The shot noise is typical of the diode that works as a barrier that can be crossed only if the electrons have an adequate energy. Not every electron has the adequate energy to cross the barrier, only a random percentage. The current becomes a random phenomenon [20]. The shot noise is given by:

$$I_{noise}(rms) = (2qI\Delta f)^{\frac{1}{2}}$$

q: electron charge ($1.6 \times 10^{-19} Coulomb$)
I: rms AC current or DC current depending upon the circuit [A]
Δf : the bandwidth [Hz]

4.3.3 Flicker Noise

The flicker noise is a phenomenon that has a density of noise power not constant but with a trend which grows with decreasing frequency (1/f) [20]. This noise is intrinsic in many electronic devices such as all systems with ion fluxes in a fluid.

4.4 PCB Design

To measure the biochip impedance a lock-in amplifier was used for the reasons described previously. To create a PCB project based on an Lock-in amplifier Altium Designer was used. Altium Designer is an electronic design automation software package for printed circuit board. The design of the PCB follows the previously described block diagram.

4.4.1 PCB Routing

The steps followed to create the PCB and output files are the following:

- Drawing the Schematic: design of the circuit pattern with the use of libraries to choose from the various components. For each component, there is a corresponding footprint
- Wiring up the Circuit: wiring is the process of creating connectivity between the various components of circuit
- Nets List: Each set of component pins that you have connected to each other now form what is referred to as a net
- Compiling the Project: Compiling a project checks for drafting and electrical rules errors in the design documents and puts you into a debugging environment
- Creating a New PCB: need to create the blank PCB with at least a board outline
- Designing the PCB: start placing the components on the PCB and routing the board

- Grids: need to ensure that our placement grid is set correctly before we start positioning the components
- Manually Routing the Board: Routing is the process of laying tracks and vias on the board to connect the components.
- Setting Up New Design Rules: Altium Designer monitors each action and checks to see if the design still complies with the design rules
- Verifying Your Board Design: Altium Designer provides a rules-driven environment in which to design PCBs and allows you to define many types of design rules to ensure the integrity of your board
- Output Documentation
  - Assembly Drawings: component positions and orientations for each side of the board
  - Composite Drawings: the finished board assembly, including components and tracks
  - PCB 3D Prints: views of the board from a three-dimensional perspective view (Fig. 4.4)

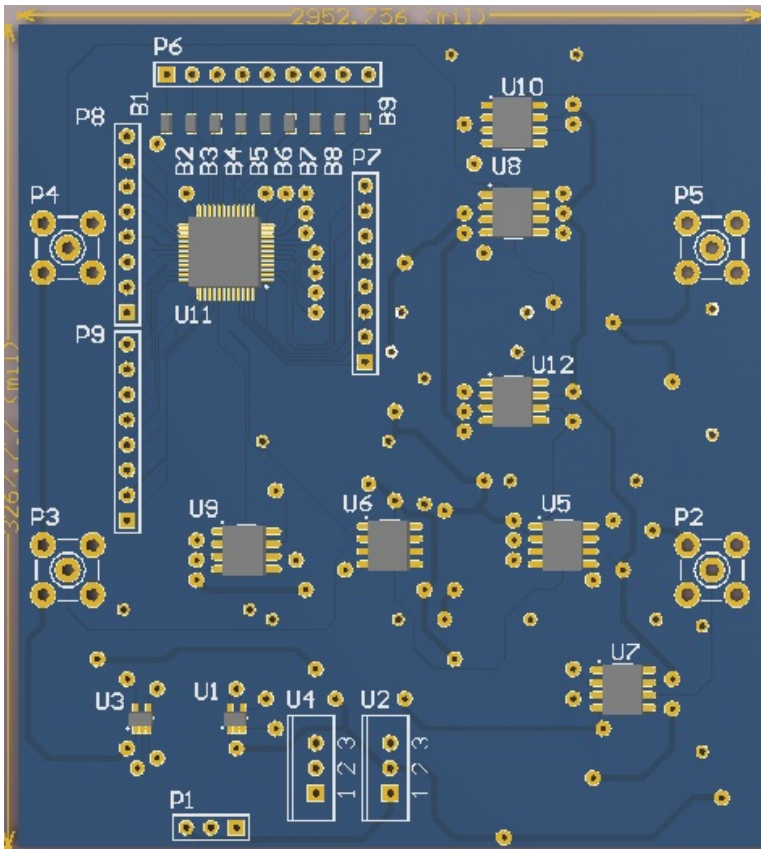

Figure 4.4: PCB Top-layer Lock-in amplifier

- Fabrication Outputs
  - Composite Drill Drawings: drill positions and sizes for the board in one drawing
  - Drill Drawing/Guides: drill positions and sizes for the board in separate drawings
  - Gerber Files: creates manufacturing information in Gerber format
  - NC Drill Files: creates manufacturing information for use by numerically controlled drilling machines
  - Solder/Paste Mask Prints: creates solder mask and paste mask drawings
- Netlist Outputs: Netlists describe the logical connectivity between components in the design and is useful for transporting to other electronics design applications.
- Bill of Materials: creates a list of parts and quantities, in various formats, required to manufacture the board (Fig. 4.5)

Comment	Description	Designator	Footprint	LibRef	Quantity
Res3	Resistor	B1, B2, B3, B4, B5, B6, B	J1-0603	Res3	13
Cap Semi	Capacitor (Semiconduct	C1, C2, C3, C4, C5, C6, C	C1206	Cap Semi	56
Cap Pol3	Polarized Capacitor (Sur	C7, C11, C13, C33	C0805	Cap Pol3	4
Header 3	Header, 3-Pin	P1	HDR1X3	Header 3	1
SMB	SMB Straight Connector	P2, P3, P4, P5	SMB_V-RJ45	SMB	4
Header 9	Header, 9-Pin	P6	HDR1X9	Header 9	1
Header 8	Header, 8-Pin	P7, P8, P9	HDR1X8	Header 8	3
Res Semi	Semiconductor Resistor	R3, R4, R5, R8, R9, R10,	AXIAL-0.5	Res Semi	10
TPS72325		U1, U3	MAA05A_M	Component_1	2
MC7805CT	Positive-Voltage Regula	U2	KC03	µA7815CKC	1
MC7905CT	Positive-Voltage Regula	U4	KC03	µA7815CKC	1
AD835AR	250MHz, Voltage Outpu	U5, U8	R-8_N	AD835AR	2
AD8031AR	High-Performance Oper	U6	D008_L	LM201ADR	1
BB627	High-Performance Oper	U7, U10	D008_L	LM201ADR	2
LMH6624	Single/ Dual Ultra Low N	U9, U12	M08A_N	LMH6624MA/NOPB	2
ADG726		U11	VBH48A_L	ADG726	1

Figure 4.5: Bill of materials

4.4.2 Working Principle

The working principle of the PCB, that it will build to measure the biochip impedance, is based on the block diagram relative to detection of a complex impedance by Lock-in amplifier (Fig. 4.6). The working principle is the following: The signal S-in goes in input to the buffer and the signal S-in-90 goes in input to the multiplier. We need two signals as we want to do the quadrature detection of the output signal from the biochip. In this way we obtain two signals in output and with this two signals, S-out and S-out-90, we can measure the magnitude and phase of the biochip impedance without the problem where modulating and demodulating signals should not be well synchronized. To generate the signals input a generator function was used where it was possible to set the form, the amplitude, the frequency, the phase of the wave.

The output signal from the buffer goes as input to the multiplexer. With this signal in input the multiplexer, controlled the DAQ, switches the channel that will be the input signal for the biochip. This signal induces a potential difference between dot and ring electrodes and between the straight electrodes that it generates an output signal current that in the first case it allows to measure the cells impedance and in the second case it allows to measure the medium's conductivity so that we can understand if there was a change in temperature of the medium.

The output signal current comes back from the biochip to the multiplexer. From the multiplexer the signal is before converted to voltage by current/voltage converter and then is amplified by an inverter amplifier. The output signal from inverter amplifier goes as input to the other multiplier. Now we have two signal: one relative to in-phase signal in input to the multiplier and a second relative to out-phase in input to the second multiplier. The multipliers modulate the signals.

The output signals from multipliers go as input to two low-pass filter with the same cut-off frequency, 0.1Hz. At the end the signals, S-out and S-out-90 from the low pass filter are manipulated by DAQ so that we can obtain the value of the biochip impedance.

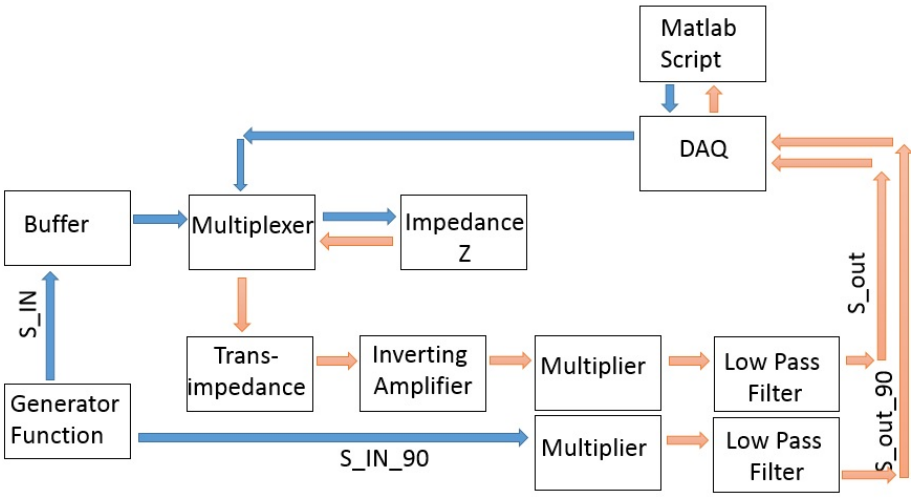

Figure 4.6: Block Diagram of the PCB

The multiplexer (Fig. 4.7 shown the schematic circuit and Appendix 2 the Datasheet) is controlled by a data acquisition (DAQ) with a script written in Matlab. The multiplexer was designed with 48 pins in particular 8 relative to the input signals and 16 relative to the output signals. A multiplexer with 8 input signals was enough as we want to measure the impedance and the medium's conductivity but the ring electrode and one from straight electrodes are the same potential when the signal input is applied.

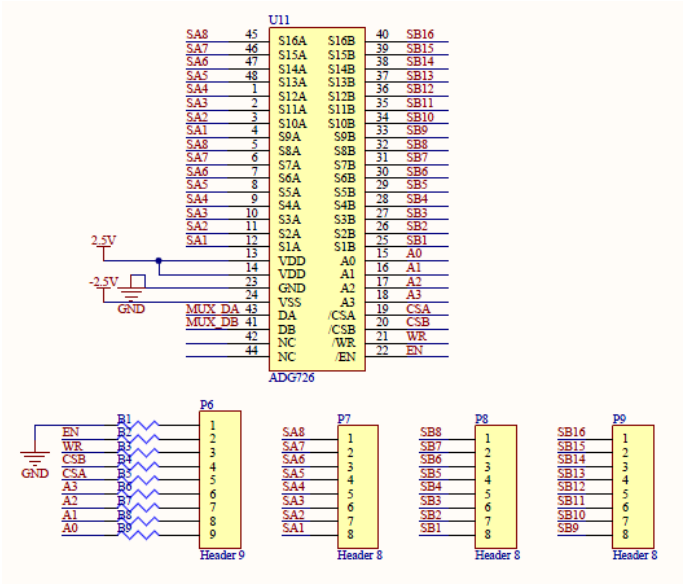

Figure 4.7: Schematic circuit of the Multiplexer ADG726. In this figure there are also the Headers that are connected with the Multiplexer as the Header for the DAQ (Header 9), the Header relative to the input signals (Header 7) and that one for the output signals (Header 8 and Header 9)

We want to measure the conductivity of the medium because when we have a change of the temperature, the conductivity of the medium changes and with this also the impedance will change. The relation between temperature and conductivity is: when the temperature changes of $\pm 1°C$ the conductivity changes almost of the 2%. With the values of the cells monolayer impedance and medium's conductivity we can understand the real value of the impedance of the cells because we know when the impedance changes due to the change in temperature of the medium, or because there was actually a change of cells impedance.

The DAQ manages the multiplexer in the following way: The DAQ is connected with a Matlab Script. The Matlab Script sends a digital signal to the DAQ. The DAQ converts this digital signal in an analog signal. The analog signal goes to the multiplexer that will act at the physical level to close and to open the right switches so that it opens the right channel in input and in output and it keeps the other channels closed. So the output signal from the multiplexer creates a potential difference on a specific biochip. The biochip generates the analog output signal which passes from the one first open channel of the multiplexer and after it goes to the DAQ that converts its into a digital signal so that it can be manipulated by a software.

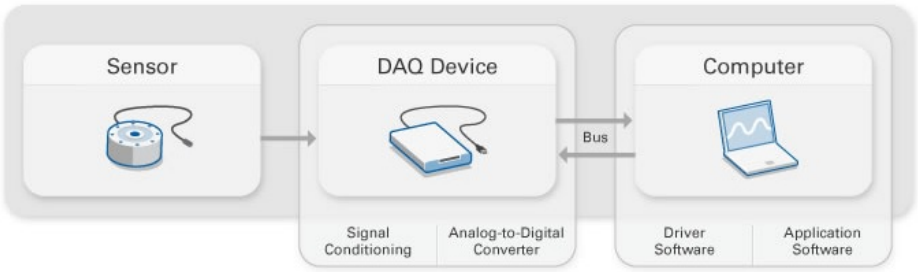

Figure 4.8: Part of a DAQ system

4.4.3 Lock-in Amplifier Simulation

The Lock-in amplifier Simulations allow to check the behavior of the circuit, the choice of the components and the values of resistors and capacitors before that the PCB is printed. The simulations were done with Altium Designer and in particular setting the components mode SPICE.

The input signal from the generator function goes in input to the buffer and then in input to the multiplexer. A buffer amplifier is used to transfer a voltage from a first circuit, having a high output impedance level, to a second circuit with a low input impedance level. The interposed buffer amplifier prevents the second circuit from loading the first circuit unacceptably and interfering with its desired operation.

The Multiplexer switches the right channel so that the input signal interacts with the biochip as explained above. The output signal from the biochip comes back before to the multiplexer and then it goes in input to the circuit that it allows the measure of the biochip impedance.

The first circuit necessary to measure the impedance is a transimpedance amplifier inverting [21]. The role of the transimpedance is to convert the signal from current to voltage. Also the transimpedance amplifies the signal 1000 times and it introduces a phase shift of 180°. The value of the output signal from the transimpedance is divided by a voltage divider composed of a resistor of $3K\Omega$ and two parallel resistors of values $3K\Omega$ and $1K\Omega$ so that the signal arrives at the input of an inverting amplifier with an amplitude decrease of 1/5. The reason for this other inverting amplifier is to introduce a phase shift to the signal of further 180° so that the measured signal will have a phase displacement that depends only of the impedance. Also this stage allows to amplify the signal of 3 times so the total gain of the circuit will be 600. The choice of this gain has been suggested as the impedance that intended to be measured have values comprised between 200Ω and $3K\Omega$. The input signal has an amplitude of 100mV so the values of the current that they has to be amplified will be comprise between 50 mA and $50\mu A$.

The operation amplifier chosen to build the two stages described above is LMH6624 of the Texas Instruments (Appendix 3). The figures 4.9, 4.10 shown respectively the transimpedance, inverting amplifier.

Transimpedance amplifier is inversely proportional to the gain set by the feedback resistor. The product of the gain is very close to being a constant for any given opamp. In Fig. 4.8 we can see the capacitor C56 where across the input terminals of the opamp introduces a low-pass filter in the feedback path. The low pass response of this filter can be characterized as the feedback factor β, which attenuates the feedback signal. This places a greater demand on the amplifier gain. The same consideration applies to inverting amplifier.

$$\beta = \frac{1}{1 + R5C56s}$$

At low frequencies the feedback factor β has little effect on the amplifier response. The amplifier response will be close to the ideal,

$$Vout = -IR5$$

where I is the current in input to the transimpedance.

In Fig. 4.9 and 4.10 we can see that between ground and the non inverting input of op amp there is a coupling capacitors. The coupling capacitors in AC has the function of allowing the transfer of the only alternate signal between two stages, preventing the passage of the continuous component. The effect of these capacitors is to form a high-pass filter, where the cutoff frequency of the filter is calculated to ensure the passage without considerable attenuation of the entire bandwidth of the signal that is intended to transfer.

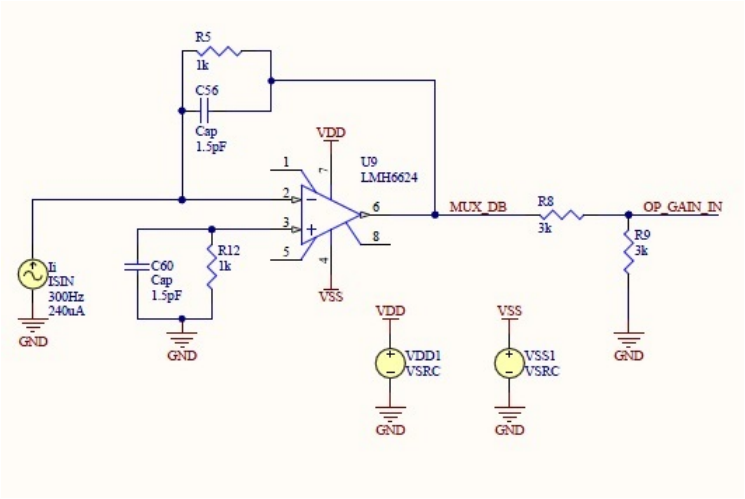

Figure 4.9: Biochip equivalent circuit model and schematic circuit Transimpedance

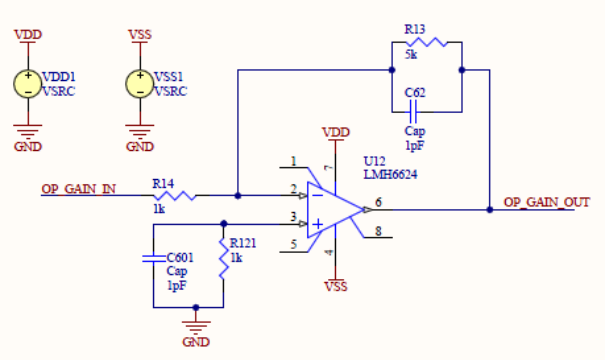

Figure 4.10: Schematic circuit Amplifier inverting

The figure 4.11 shows the simulation of the first part of the PCB when the impedance that you want to measure, for example, is relative to the biochip with the cells not treated with the reagents. The value of this impedance is almost 466Ω so the current in input to the transimpedance will be $240\mu A$. The complex impedance introduces a phase shift of 17°. In particular we can see the plots relative to the signal that we have after the transimpedance and the amplifier inverting. The signal is converted from current to voltage and amplified.

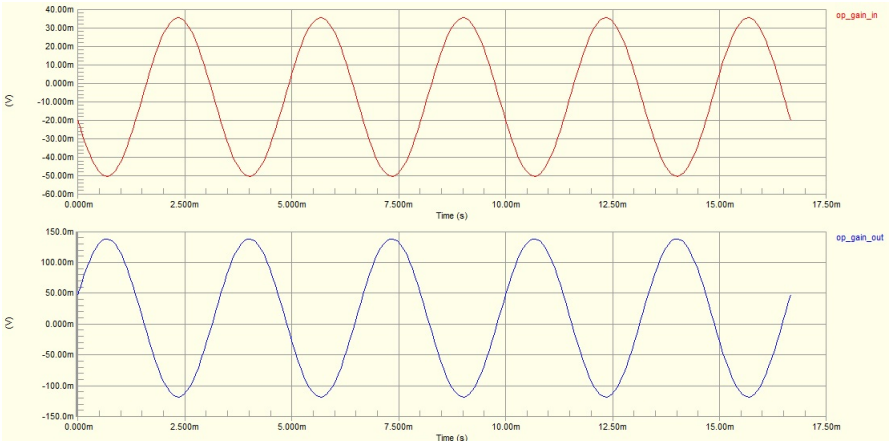

Figure 4.11: op-gain-IN: output signal from transimpedance, op-gain-OUT: output signal from amplifier inverting

The output signal from the amplifier inverting goes in input to two multipliers where in a case the output signal is multiplied with the input signal with phase zero and in the other case the output signal is multiplied with the input signal but the signal is phase shifted by 180°. In this way we have two outputs: one proportional to $\cos(\theta)$ and the other proportional to $\sin(\theta)$ so the two signals from the multipliers are always synchronized regardless of the value of impedance to be measured (Fig. 4.12).

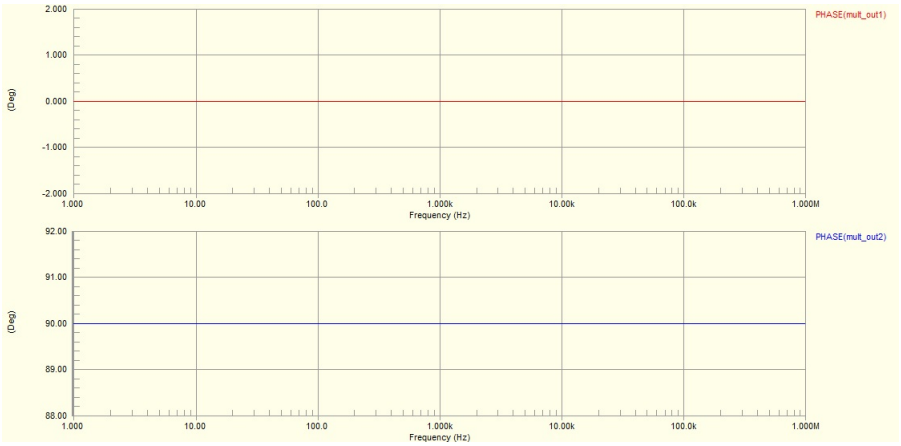

Figure 4.12: Phase of the output signals from Multipliers

The choosen multipliers are AD835 of Analag Device (Appendix 4). The Datasheet describes the possibility to add in the feedback a voltage divider with resistance values of 200Ω and $2K\Omega$ so that the gain adjusted of 10% in the case where there are losses in the circuit. The Fig. 4.13 shows the schematic circuit of multipliers.

In the figure 4.14 we can see the simulation relative to the multiplied and in particular we can see that the output signals from the multipliers are always of a phase displacement of 90°.

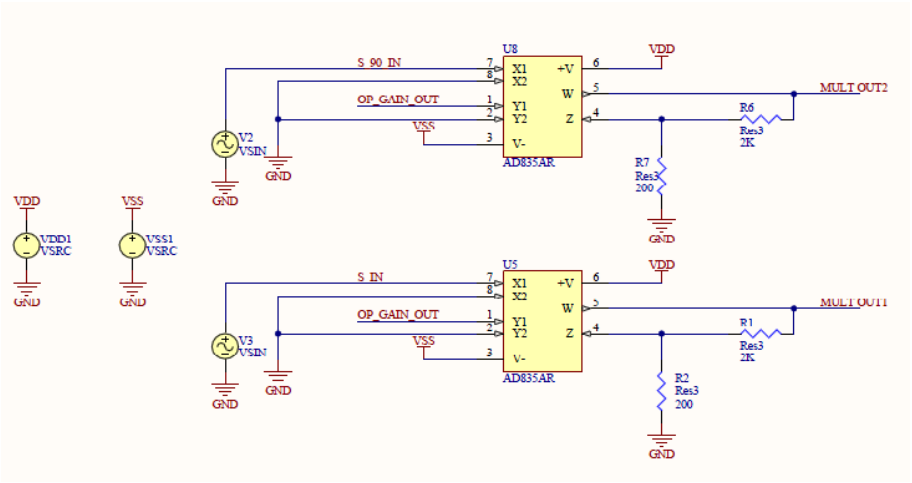

Figure 4.13: Schematic circuit Multipliers

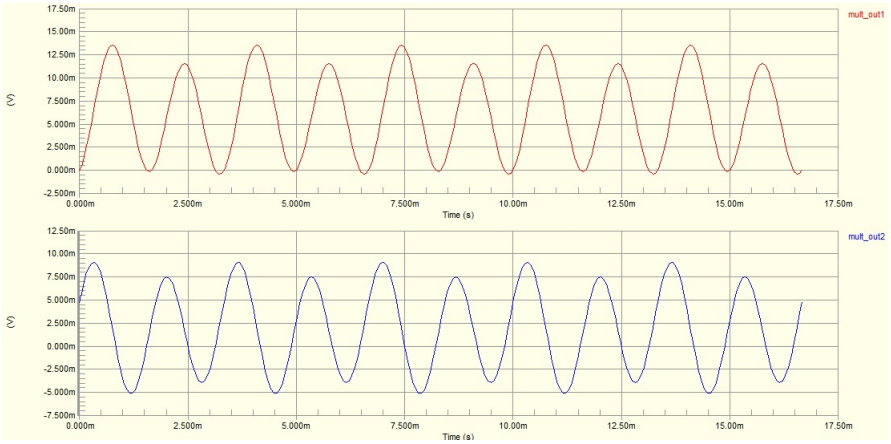

Figure 4.14: Output signals from the multipliers

The last step of the circuit is relative to the filtering of the signals from the multipliers to obtain the DC signal so that we can get the real part and the complex part of the impedance and then to calculate its magnitude and phase. In order to obtain a DC output, a low-pass filter is needed to remove the spikes. In this design, a two pole active filter was chosen, using the Sallen-Key filter structure configured as a Butterworth low-pass filter [22]. OPA627 (Appendix 5) is the op amp used for the active low-pass filter; and the gain of the filter is about 1; the cut off frequency of the low pass-filter is set to about 0.1Hz. In figure 4.15 there is the Schematic of the low-pass filter.

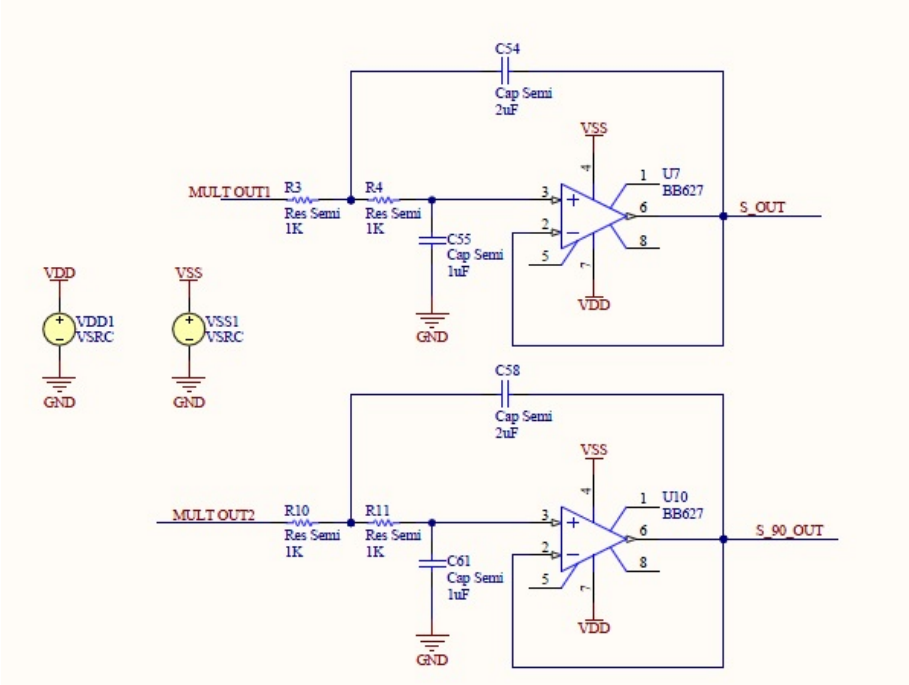

Figure 4.15: Schematic circuit Filters

The SPICE simulation of the step relative to the low pass filter is shown in figure 4.16.

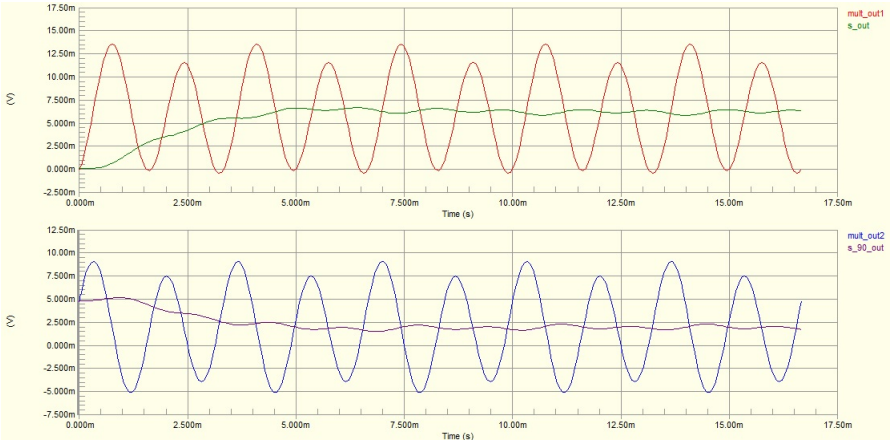

Figure 4.16: DC output

With the real part and the complex part we can calculate the magnitude and phase of the impedance. We can check the operation of the circuit by comparing the values of magnitude and phase with the values obtained from a simulation with ZView (Fig. 4.17).

With Zview the Equivalent Circuit Model was simulated. The values of magnitude and phase of the impedance were obtained. The value of current was calculated with Ohms law. The value current was put in input to the transimpedance. The values of real part (x) and imaginary part (y) were obtained with the circuit simulation. The values of magnitude and phase were calculated using x and y.

$$x = 6.25mV$$

$$y = 1.9mV$$

$$\frac{A^2G}{\sqrt{x^2+y^2}} = 465\Omega$$

$$\arctan\left(\frac{y}{x}\right) = 16.9^\circ$$

These values are the same obtained with the simulation made with Zview.

In the same way, we can compare the results of the simulation when we want to measure the impedance belonging to the biochip without cells (Fig. 4.18). The value of magnitude in ZView is 294Ω and the phase is 21.6°. The value of real part from the DC signal from the simulation circuit is 3.4mV and the value of complex part is 10.23mV. So the value of the magnitude is 292.3Ω and the value of the phase is 21.3°. When the impedance changes in input to the circuit the value of the gain doesn't change.

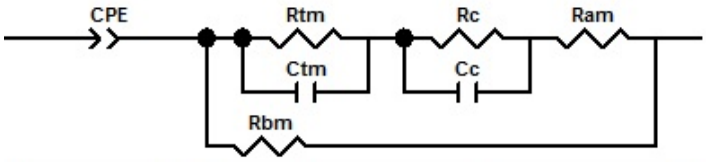

Element	Freedom	Value	Error	Error%
CPE-T	Fixed	0.00015	N/A	N/A
CPE-P	Fixed	0.5	N/A	N/A
Rtm	Fixed	48	N/A	N/A
Ctm	Fixed	4.700E-11	N/A	N/A
Rc	Fixed	835	N/A	N/A
Cc	Fixed	2.47E-7	N/A	N/A
Ram	Fixed	198	N/A	N/A
Rbm	Fixed	500	N/A	N/A

Figure 4.17: Equivalent circuit model ZView

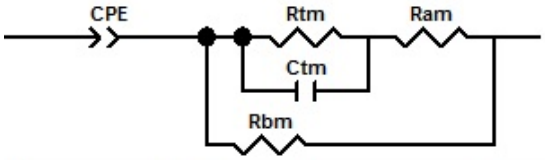

Element	Freedom	Value	Error	Error%
CPE-T	Fixed	0.00015	N/A	N/A
CPE-P	Fixed	0.5	N/A	N/A
Rtm	Fixed	48	N/A	N/A
Ctm	Fixed	4.700E-11	N/A	N/A
Ram	Fixed	198	N/A	N/A
Rbm	Fixed	500	N/A	N/A

Figure 4.18: Equivalent circuit model ZView without cells

In fig. 4.19 we can see the bottom layer of PCB where was used a stage capacitive decoupling. Decoupling has been defined as the art and practice of separation and removal of undesirable coupling portions of circuits and systems to ensure proper operation. Therefore, decoupling the power to the various elements of the circuit means cancelling or limiting the effect of the instant demand of current. While the load is inactive, the capacitor is charged to full supply voltage; when the load is applied, the capacitor provides the initial pulse of current.

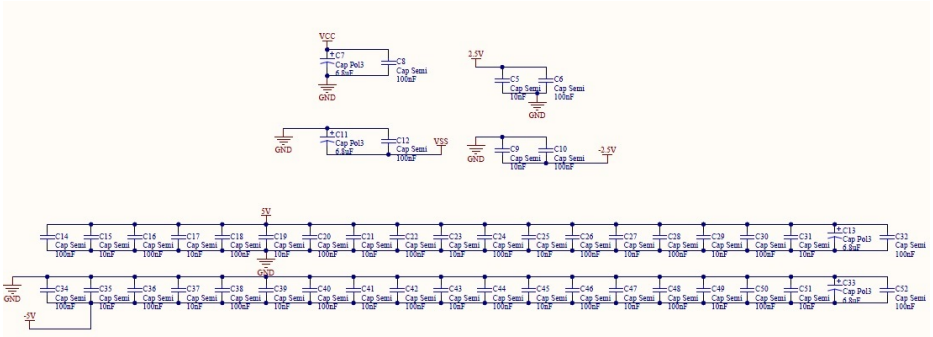

Figure 4.19: Bottom Layer PCB: Capacitive Decoupling

4.4.4 Matlab Script

The multiplexer is managed by the DAQ. The DAQ is programmed with a Matlab Script where using of Matlab functions it is possible to create a session so that the signals are generated to control the multiplexer and starting a measurement of a channel relative to the biochip. The channels of the multiplexer are controlled by the DAQ that sends the digital signals to close and to open them. The DAQ is programmed by Matlab Script. In particular the digital signals, that comes in input from the DAQ, are based on a true table describes on the Datasheet of the multiplexer.

The output signals from the biochip are filtered with a filter average so that we can cut the ripple of DC output. With this values and with the formulas describe above, we can calculate and plot the values of the biochip impedance. Also with the Matlab Script it is possible to set same parameters before to start the measures. In particular we can set the interval of time between two measurements of the same biochip and we can set the numbers of scan for a single channel.

In this Script there is the control relative to measures of medium conductivity. In particular for a single channel we can measure the magnitude of the biochip impedance and also the medium conductivity so that we can calculate the real value of the cells resistance subtracting the value of the impedance due to the change in temperature of the medium with those relative to change of the cells monolayer impedance.

4.5 Chip to World Connection

The Biochip has to stay in an incubator as cells have to be maintained alive for a long period. However, the electronics part can't stay in an incubator as the circuits are sensitive at the humidity. The solution to this problem has been a PCB that links the input signals and the output signals from the biochips to the outside world and vice versa. The PCB was designed with Design Spark. DesignSpark PCB is a free-of-charge schematic capture and PCB layout tool for electronics design automation. The shielded ribbon wire is used to connect the biochips from inside the incubator to the electrical circuit were.

4.5.1 Design

The design of this PCB presents 4 layers where every, track passes link from the biochip to the electronic parts and vice versa. The size were dictated by the need that the PCB had to integrate with 96 wells plate. This support allowed to connect the syringe pump that permits to pump the medium to the inlet of the biochip and the fraction collector with outlet of the biochip.

The functionality of the PCB is the following: when we put the biochip on the PCB, the electrodes of the biochip make contact with piece interface (Fig. 4.20). These with their pins touch the pads that are present on the fourth layer of the PCB. In this way we can bring the signals from the biochip to the outside and vice versa and in particular we have three signals for each biochip: input signal, conductivity output signal and impedance output signal. These signals that we have on the fourth layer are brought to the connectors exploiting the other three layers. The connectors are placed on the first layer so that we can link the electronic parts with the biochips that are in the incubator.

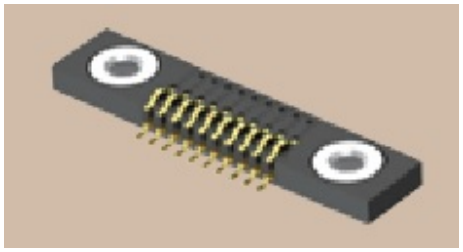

Figure 4.20: Piece Interface

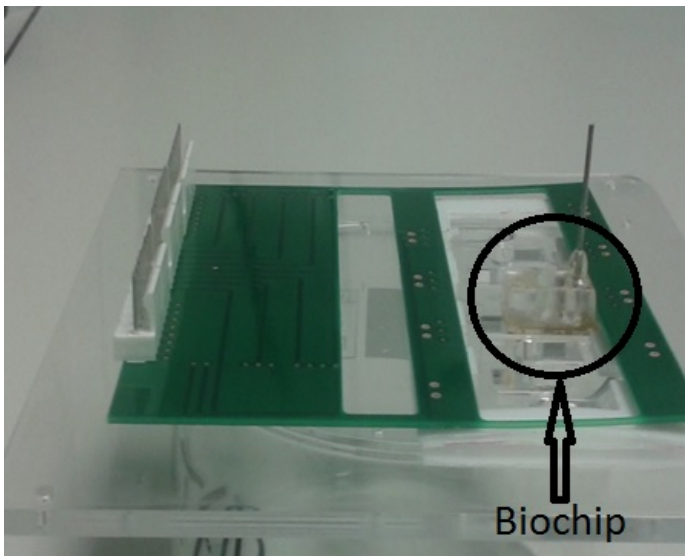

Figure 4.21: PCB design connect to biochip

Chapter 5

Conclusions

A microfluidic device was designed for monitoring the epithelial cell barrier integrity. The Equivalent Circuit Model was proposed to model the device. The Equivalent circuit Model allows to characterize the electrical properties of the cell monolayer. The values of the impedance cell layer are determined simulating the model. The behavior of the impedance was studied simulating a challenge of the cell monolayer with reagents as POLY I:C and EGTA. The impedance decrease related to the loss of epithelial tight junctions.

The simulations allow to choose the frequency of the imput signal to the device. The trend of the magnitude and phase relative to the impedance suggest a frequency of 300Hz. At this frequency the response of the system allows more accurate measurements of impedance.

The electrical double layer effect at low frequencies was reduced by black platinum deposition on platinum electrodes. The capacitance of the double layer increases so that it shield much less the electric field that allows for a interaction with the cells.

The measurements of impedance done with the Impedance Analayzer determine the behavior of the microfluidic device. The measurements confirm the validity of the Equivalent Circuit Model proposed. Also the measurements confirm a decrease in the electrical double layer effect when coated electrodes are used.

The Lock-in Amplifier was designed to measure the impedance. The circuit has the advantage that is low-cost compared to a system that measures the impedance as an Impedance Analyzer. The Lock-in Amplifier compared with system that use chopstick-electrodes or a multimeter has the advantage that is not a manual instrument and it is likely to perform continuous measurements (high temporal resolution) over 24 h or longer. Also the measurements with hand-held meter are affected by systematic errors as the measurements depend from the position where the electrodes are positioned.

Appendix 1

```
clc
clear all
close all


A_membrane=0.196;              %area membrane new model [cm^2]
A_electrodes=0.031;            %area electrodes new model [cm^2]
Ctm=47*10^-12;                 %cap membrane [F]
Rtm=48;                        %res trans membrane new model [Ohm]
Ram=198;                       %res apical medium [Ohm]
Rbm=500;                       %res baso medium [Ohm]
Cc=(1.26*10^-6)*A_membrane;    %cap cells [F]
TEER=1000;                     %[Ohm]
Rc_blank=165;                  %res without cells [Ohm]
Rc_poly=TEER-Rc_blank;         %res cells treatment poly [Ohm]
Rc_egta=TEER-Rc_blank;         %res cells treatment egta [Ohm]
C_DL=(80*10^-6)*A_electrodes;%cap double layer [F]

f=[10:20:10^5];                %freq of input signal [Hz]
h=1;
j=1;

e=input('number of pr');       %number of curves
n=[1:e];                       %at first lap got the
                                data about cells layer

T=1.5*10^-4;
p=0.5;

while j<=length(f) && h<=length(n)
```

```
w=2*pi.*f(j);                   %pulsation [rad/s]
s0=i*w;                         %imaginary pulsation
Zedl=(T*(s0)^p)^-1;             %imaginary pulsation

 %fdt with poly
Z_poly(j)=Zedl+(((((Rtm./(1+s0*Rtm*Ctm))+
  +(Rc_poly./(1+s0*Rc_poly*Cc))+Ram).^-1)+(1./Rbm)).^-1);
%fdt with egta
Z_egta(j)=Zedl+(((((Rtm./(1+s0*Rtm*Ctm))+
  +(Rc_egta./(1+s0*Rc_egta*Cc))+Ram).^-1)+(1./Rbm)).^-1);
%fdt without cells
Z_blank(j)=Zedl+(((((Rtm./(1+s0*Rtm*Ctm))+Ram).^-1)+(1./Rbm)).^-1);

%magnitude with poly
modZ_poly(h,j)=sqrt((real(Z_poly(j))).^2+(imag(Z_poly(j))).^2);
%phase with poly
phaseZ_poly(h,j)=(360/(2*pi))*(atan(imag(Z_poly(j))./real(Z_poly(j))));
%magnitude with egta
modZ_egta(h,j)=sqrt((real(Z_egta(j))).^2+(imag(Z_egta(j))).^2);
%phase with egta
phaseZ_egta(h,j)=(360/(2*pi))*(atan(imag(Z_egta(j))./real(Z_egta(j))));
%magnitude without cells
modZ_blank(j)=sqrt((real(Z_blank(j))).^2+(imag(Z_blank(j))).^2);
%phase without cells
phaseZ_blank(j)=(360/(2*pi))*(atan(imag(Z_blank(j))./real(Z_blank(j))));

%real part with poly
Z_Re_poly(h,j)=real(Z_poly(j));
%real part with egta
Z_Re_egta(h,j)=real(Z_egta(j));
%real part without cells
Z_Re_blank(j)=real(Z_blank(j));
%imaginary part with poly
Z_Im_poly(h,j)=imag(Z_poly(j));
%imaginary part with egta
Z_Im_egta(h,j)=imag(Z_egta(j));
%imaginary part new model without cells
Z_Im_blank(j)=imag(Z_blank(j));

j=j+1;
if j>length(f)
    %drop res cells with egta
    Rc_poly=Rc_poly-TEER*0.5;
    %drop res cells with poly
    Rc_egta=Rc_egta-TEER*0.8;
```

```
    j=1;
    h=h+1;
end

end


figure(1)
semilogx(f,modZ_poly(1,:),'r')
hold on
semilogx(f,modZ_poly(2,:),'b')
semilogx(f,modZ_egta(2,:),'k')
semilogx(f,modZ_blank,'g')
xlabel('Frequency [Hz]'); ylabel('Magnitude [Ohm]');
title('Equivalent circuit model no DL')
legend('confluent cell layer','POLY(I:C)
       treatment','EGTA treatment','no cell layer')


figure(2)
semilogx(f,phaseZ_poly(1,:),'r')
hold on
semilogx(f,phaseZ_poly(2,:),'b')
semilogx(f,phaseZ_egta(2,:),'k')
semilogx(f,phaseZ_blank,'g')
xlabel('Frequency [Hz]'); ylabel('Phase [Deg]');
title('Equivalent circuit model no DL')
legend('confluent cell layer','POLY(I:C)
       treatment','EGTA treatment','no cell layer')


figure(3)
semilogx(f,Z_Re_poly(1,:),'r')
hold on
semilogx(f,Z_Re_poly(2,:),'b')
semilogx(f,Z_Re_egta(2,:),'k')
semilogx(f,Z_Re_blank,'g')
xlabel('Frequency [Hz]'); ylabel('Real Part [Ohm]');
title('Real Part equivalent circuit model')
legend('confluent cell layer','POLY treatment',
       'EGTA treatment','no cell layer')


figure(4)
semilogx(f,(Z_Im_poly(1,:)),'r')
```

```
hold on
semilogx(f,(Z_Im_poly(2,:)),'b')
semilogx(f,(Z_Im_egta(2,:)),'k')
semilogx(f,(Z_Im_blank),'g')
xlabel('frequency [Hz]'); ylabel('Imaginary part [Ohm]');
title('Imaginary equivalent circuit model')
legend('confluent cell layer','POLY treatment',
       'EGTA treatment','no cell layer')
```

Appendix 2

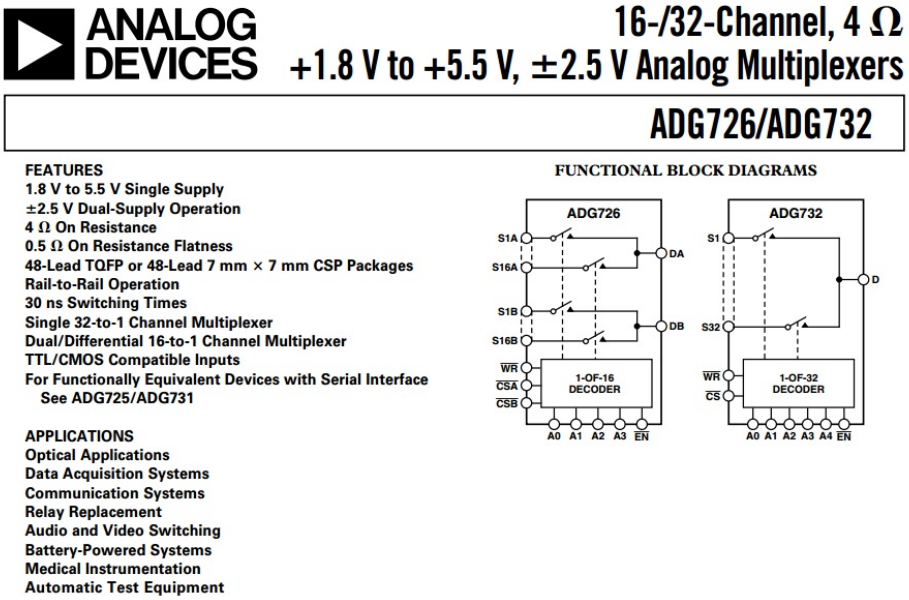

ANALOG DEVICES

16-/32-Channel, 4 Ω
+1.8 V to +5.5 V, ±2.5 V Analog Multiplexers

ADG726/ADG732

FEATURES
1.8 V to 5.5 V Single Supply
±2.5 V Dual-Supply Operation
4 Ω On Resistance
0.5 Ω On Resistance Flatness
48-Lead TQFP or 48-Lead 7 mm × 7 mm CSP Packages
Rail-to-Rail Operation
30 ns Switching Times
Single 32-to-1 Channel Multiplexer
Dual/Differential 16-to-1 Channel Multiplexer
TTL/CMOS Compatible Inputs
For Functionally Equivalent Devices with Serial Interface
See ADG725/ADG731

APPLICATIONS
Optical Applications
Data Acquisition Systems
Communication Systems
Relay Replacement
Audio and Video Switching
Battery-Powered Systems
Medical Instrumentation
Automatic Test Equipment

FUNCTIONAL BLOCK DIAGRAMS

Figure 5.1: Datasheet Multiplexer ADG726

ADG726/ADG732 SPECIFICATIONS[1]

DUAL SUPPLY (V_{DD} = +2.5 V ± 10%, V_{SS} = –2.5 V ± 10%, GND = 0 V, unless otherwise noted.)

Parameter	B Version +25°C	B Version –40°C to +85°C	Unit	Test Conditions/Comments
ANALOG SWITCH				
Analog Signal Range		V_{SS} to V_{DD}	V	
On Resistance (R_{ON})	4		Ω typ	V_S = V_{SS} to V_{DD}, I_{DS} = 10 mA;
	5.5	6	Ω max	Test Circuit 1
On Resistance Match Between		0.3	Ω typ	V_S = V_{SS} to V_{DD}, I_{DS} = 10 mA
Channels (ΔR_{ON})		0.8	Ω max	
On Resistance Flatness ($R_{FLAT(ON)}$)	0.5		Ω typ	V_S = V_{SS} to V_{DD}, I_{DS} = 10 mA
		1	Ω max	
LEAKAGE CURRENTS				V_{DD} = +2.75 V, V_{SS} = –2.75 V
Source OFF Leakage I_S (OFF)	±0.01		nA typ	V_S = +2.25 V/–1.25 V, V_D = –1.25 V/+2.25 V;
	±0.25	±0.5	nA max	Test Circuit 2
Drain OFF Leakage I_D (OFF)	±0.05		nA max	V_S = +2.25 V/–1.25 V, V_D = –1.25 V/+2.25 V;
ADG726	±0.5	±2.5	nA max	Test Circuit 3
ADG732	±1	±5	nA max	
Channel ON Leakage I_D, I_S (ON)	±0.05		nA typ	V_S = V_D = +2.25 V/–1.25 V;
ADG726	±0.5	±2.5	nA max	Test Circuit 4
ADG732	±1	±5	nA max	
DIGITAL INPUTS				
Input High Voltage, V_{INH}		1.7	V min	
Input Low Voltage, V_{INL}		0.7	V max	
Input Current				
I_{INL} or I_{INH}	0.005		µA typ	V_{IN} = V_{INL} or V_{INH}
		±0.5	µA max	
C_{IN}, Digital Input Capacitance	5		pF typ	
DYNAMIC CHARACTERISTICS[2]				
$t_{TRANSITION}$	33		ns typ	R_L = 300 Ω, C_L = 35 pF; Test Circuit 5
	45	51	ns max	V_{S1} = 1.5 V/0 V, V_{S2} = 0 V/1.5 V
Break-Before-Make Time Delay, t_D	15		ns typ	R_L = 300 Ω, C_L = 35 pF;
	1		ns min	V_S = 1.5 V; Test Circuit 6
t_{ON}($\overline{CS}$, $\overline{WR}$)	21		ns typ	V_S = 1.5 V; Test Circuit 7
	30	37	ns max	R_L = 300 Ω, C_L = 35 pF;
t_{OFF}($\overline{CS}$, $\overline{WR}$)	20		ns typ	V_S = 1.5 V; Test Circuit 7
	29	35	ns max	R_L = 300 Ω, C_L = 35 pF;
t_{ON}($\overline{EN}$, $\overline{WR}$)	26		ns typ	R_L = 300 Ω, C_L = 35 pF;
	37		ns max	V_S = 1.5 V; Test Circuit 8
t_{OFF}($\overline{EN}$)	18		ns typ	R_L = 300 Ω, C_L = 35 pF;
	26	29	ns max	V_S = 1.5 V; Test Circuit 8
Charge Injection	1		pC typ	V_S = 0 V, R_S = 0 Ω, C_L = 1 nF; Test Circuit 9
OFF Isolation	–72		dB typ	R_L = 50 Ω, C_L = 5 pF, f = 1 MHz; Test Circuit 10
Channel-to-Channel Crosstalk	–72		dB typ	R_L = 50 Ω, C_L = 5 pF, f = 1 MHz; Test Circuit 11
–3 dB Bandwidth				R_L = 50 Ω, C_L = 5 pF; Test Circuit 12
ADG726	34		MHz typ	
ADG732	18		MHz typ	
C_S (OFF)	13		pF typ	
C_D (OFF)				
ADG726	137		pF typ	f = 1 MHz
ADG732	275		pF typ	f = 1 MHz
C_D, C_S (ON)				
ADG726	150		pF typ	f = 1 MHz
ADG732	300		pF typ	f = 1 MHz
POWER REQUIREMENTS				
I_{DD}	10		µA typ	V_{DD} = +2.75 V
		20	µA max	Digital Inputs = 0 V or +2.75 V
I_{SS}	10		µA typ	V_{SS} = –2.75 V
		20	µA max	Digital Inputs = 0 V or +2.75 V

NOTES

[1]Temperature range is as follows: B Version: –40°C to +85°C.

[2]Guaranteed by design; not subject to production test.

Specifications subject to change without notice.

Table I. ADG726 Truth Table

A3	A2	A1	A0	$\overline{EN}$	$\overline{CSA}$	$\overline{CSB}$	$\overline{WR}$	ON Switch
X	X	X	X	X	1	1	L->H	Retains Previous Switch Condition
X	X	X	X	X	1	1	X	No Change in Switch Condition
X	X	X	X	1	0	0	0	NONE
0	0	0	0	0	0	0	0	S1A–DA, S1B–DB
0	0	0	1	0	0	0	0	S2A–DA, S2B–DB
0	0	1	0	0	0	0	0	S3A–DA, S3B–DB
0	0	1	1	0	0	0	0	S4A–DA, S4B–DB
0	1	0	0	0	0	0	0	S5A–DA, S5B–DB
0	1	0	1	0	0	0	0	S6A–DA, S6B–DB
0	1	1	0	0	0	0	0	S7A–DA, S7B–DB
0	1	1	1	0	0	0	0	S8A–DA, S8B–DB
1	0	0	0	0	0	0	0	S9A–DA, S9B–DB
1	0	0	1	0	0	0	0	S10A–DA, S10B–DB
1	0	1	0	0	0	0	0	S11A–DA, S11B–DB
1	0	1	1	0	0	0	0	S12A–DA, S12B–DB
1	1	0	0	0	0	0	0	S13A–DA, S13B–DB
1	1	0	1	0	0	0	0	S14A–DA, S14B–DB
1	1	1	0	0	0	0	0	S15A–DA, S15B–DB
1	1	1	1	0	0	0	0	S16A–DA, S16B–DB

X = Don't Care

Table II. ADG732 Truth Table

A4	A3	A2	A1	A0	$\overline{EN}$	$\overline{CS}$	$\overline{WR}$	Switch Condition
X	X	X	X	X	X	1	L->H	Retains Previous Switch Condition
X	X	X	X	X	X	1	X	No Change in Switch Condition
X	X	X	X	X	1	0	0	NONE
0	0	0	0	0	0	0	0	1
0	0	0	0	1	0	0	0	2
0	0	0	1	0	0	0	0	3
0	0	0	1	1	0	0	0	4
0	0	1	0	0	0	0	0	5
0	0	1	0	1	0	0	0	6
0	0	1	1	0	0	0	0	7
0	0	1	1	1	0	0	0	8
0	1	0	0	0	0	0	0	9
0	1	0	0	1	0	0	0	10
0	1	0	1	0	0	0	0	11
0	1	0	1	1	0	0	0	12
0	1	1	0	0	0	0	0	13
0	1	1	0	1	0	0	0	14
0	1	1	1	0	0	0	0	15
0	1	1	1	1	0	0	0	16
1	0	0	0	0	0	0	0	17
1	0	0	0	1	0	0	0	18
1	0	0	1	0	0	0	0	19
1	0	0	1	1	0	0	0	20
1	0	1	0	0	0	0	0	21
1	0	1	0	1	0	0	0	22
1	0	1	1	0	0	0	0	23
1	0	1	1	1	0	0	0	24
1	1	0	0	0	0	0	0	25
1	1	0	0	1	0	0	0	26
1	1	0	1	0	0	0	0	27
1	1	0	1	1	0	0	0	28
1	1	1	0	0	0	0	0	29
1	1	1	0	1	0	0	0	30
1	1	1	1	0	0	0	0	31
1	1	1	1	1	0	0	0	32

X = Don't Care

Appendix 3

LMH6624 and LMH6626 Single/Dual Ultra Low Noise Wideband Operational Amplifier

1 Features

- V_S = ±6 V, T_A = 25°C, A_V = 20 (Typical Values Unless Specified)
- Gain Bandwidth (LMH6624) 1.5 GHz
- Input Voltage Noise 0.92 nV/√Hz
- Input Offset Voltage (limit over temp) 700 µV
- Slew Rate 350 V/µs
- Slew Rate (A_V = 10) 400 V/µs
- HD2 at f = 10 MHz, R_L = 100 Ω −63 dBc
- HD3 at f = 10 MHz, R_L = 100 Ω −80 dBc
- Supply Voltage Range (Dual Supply) 2.5 V to 6 V
- Supply Voltage Range (Single Supply) 5 V to 12 V
- Improved Replacement for the CLC425 (LMH6624)
- Stable for Closed Loop $|A_V| \geq 10$

2 Applications

- Instrumentation Sense Amplifiers
- Ultrasound Pre-amps
- Magnetic Tape & Disk Pre-amps
- Wide Band Active Filters
- Professional Audio Systems
- Opto-electronics
- Medical Diagnostic Systems

3 Description

The LMH6624 and LMH6626 devices offer wide bandwidth (1.5 GHz for single, 1.3 GHz for dual) with very low input noise (0.92 nV/√Hz, 2.3 pA/√Hz) and ultra-low dc errors (100 µV V_{OS}, ±0.1 µV/°C drift) providing very precise operational amplifiers with wide dynamic range. This enables the user to achieve closed-loop gains of greater than 10, in both inverting and non-inverting configurations.

The LMH6624 (single) and LMH6626 (dual) traditional voltage feedback topology provide the following benefits: balanced inputs, low offset voltage and offset current, very low offset drift, 81dB open loop gain, 95dB common mode rejection ratio, and 88dB power supply rejection ratio.

The LMH6624 and LMH6626 devices operate from ±2.5 V to ±6 V in dual supply mode and from 5 V to 12 V in single supply configuration.

LMH6624 is offered in SOT-23-5 and SOIC-8 packages. The LMH6626 is offered in SOIC-8 and VSSOP-8 packages.

Device Information[1]

PART NUMBER	PACKAGE	BODY SIZE (NOM)
LMH6624	SOT-23 (5)	2.90 mm × 1.60 mm
	SOIC (8)	4.90 mm × 3.91 mm
LMH6626	SOIC (8)	4.90 mm × 3.91 mm
	VSSOP (8)	3.00 mm × 3.00 mm

Figure 5.2: Datasheet Operational Amplifier LMH6624

6.6 Electrical Characteristics ±6 V

Unless otherwise specified, all limits ensured at T_A = 25°C, V^+ = 6 V, V^- = −6 V, V_{CM} = 0 V, A_V = +20, R_F = 500 Ω, R_L = 100 Ω. See (1).

PARAMETER		TEST CONDITIONS		MIN(2)	TYP(3)	MAX(2)	UNIT
DYNAMIC PERFORMANCE							
f_{CL}	−3dB BW	V_O = 400 mV_{PP} (LMH6624)			95		MHz
		V_O = 400 mV_{PP} (LMH6626)			85		
SR	Slew rate(4)	V_O = 2 V_{PP}, A_V = +20 (LMH6624)			350		V/µs
		V_O = 2 V_{PP}, A_V = +20 (LMH6626)			320		
		V_O = 2 V_{PP}, A_V = +10 (LMH6624)			400		
		V_O = 2 V_{PP}, A_V = +10 (LMH6626)			360		
t_r	Rise time	V_O = 400 mV Step, 10% to 90%			3.7		ns
t_f	Fall time	V_O = 400 mV Step, 10% to 90%			3.7		ns
t_s	Settling time 0.1%	V_O = 2 V_{PP} (Step)			18		ns
DISTORTION and NOISE RESPONSE							
e_n	Input referred voltage noise	f = 1 MHz (LMH6624)			0.92		nV/√Hz
		f = 1 MHz (LMH6626)			1.0		
i_n	Input referred current noise	f = 1 MHz (LMH6624)			2.3		pA/√Hz
		f = 1 MHz (LMH6626)			1.8		
HD2	2nd harmonic distortion	f_C = 10 MHz, V_O = 1 V_{PP}, R_L = 100 Ω			−63		dBc
HD3	3rd harmonic distortion	f_C = 10 MHz, V_O = 1 V_{PP}, R_L = 100 Ω			−80		dBc
INPUT CHARACTERISTICS							
V_{OS}	Input offset voltage	V_{CM} = 0 V		−0.5	±0.10	+0.5	mV
			-40°C ≤ T_J ≤ 125°C	−0.7		+0.7	
	Average drift(5)	V_{CM} = 0 V			±0.2		µV/°C
I_{OS}	Input offset current	(LMH6624) V_{CM} = 0 V		−1.1	0.05	1.1	µA
			-40°C ≤ T_J ≤ 125°C	−2.5		2.5	
		(LMH6626) V_{CM} = 0 V		−2.0	0.1	2.0	
			-40°C ≤ T_J ≤ 125°C	−2.5		2.5	
	Average drift(5)	V_{CM} = 0 V			0.7		nA/°C
I_B	Input bias current	V_{CM} = 0 V			13	+20	µA
			-40°C ≤ T_J ≤ 125°C			+25	
	Average drift(5)	V_{CM} = 0 V			12		nA/°C
R_{IN}	Input resistance(6)	Common Mode			6.6		MΩ
		Differential Mode			4.6		kΩ
C_{IN}	Input capacitance(6)	Common Mode			0.9		pF
		Differential Mode			2.0		
CMRR	Common mode rejection ratio	Input Referred, V_{CM} = −4.5 to +5.25 V		90	95		dB
		Input Referred, V_{CM} = −4.5 to +5.0 V	-40°C ≤ T_J ≤ 125°C	87			

(1) Electrical table values apply only for factory testing conditions at the temperature indicated. Factory testing conditions result in very limited self-heating of the device such that T_J = T_A. No ensured specification of parametric performance is indicated in the electrical tables under conditions of internal self-heating where T_J > T_A. Absolute maximum ratings indicate junction temperature limits beyond which the device may be permanently degraded, either mechanically or electrically.
(2) All limits are specified by testing or statistical analysis.
(3) Typical Values represent the most likely parametric norm.
(4) Slew rate is the slowest of the rising and falling slew rates.
(5) Average drift is determined by dividing the change in parameter at temperature extremes into the total temperature change.
(6) Simulation results.

Electrical Characteristics ±6 V (continued)

Unless otherwise specified, all limits ensured at T_A = 25°C, V^+ = 6 V, V^- = −6 V, V_{CM} = 0 V, A_V = +20, R_F = 500 Ω, R_L = 100 Ω. See (1).

PARAMETER		TEST CONDITIONS		MIN(2)	TYP(3)	MAX(2)	UNIT
TRANSFER CHARACTERISTICS							
A_{VOL}	Large signal voltage gain	(LMH6624) R_L = 100 Ω, V_O = −3 V to +3 V		77	81		dB
			-40°C ≤ T_J ≤ 125°C	72			
		(LMH6626) R_L = 100 Ω, V_O = −3 V to +3 V		74	80		
			-40°C ≤ T_J ≤ 125°C	70			
X_t	Crosstalk rejection	f = 1MHz (LMH6626)			−75		dB
OUTPUT CHARACTERISTICS							
V_O	Output swing	(LMH6624) R_L = 100 Ω		±4.4	±4.9		V
			-40°C ≤ T_J ≤ 125°C	±4.3			
		(LMH6624) No Load		±4.8	±5.2		
			-40°C ≤ T_J ≤ 125°C	±4.65			
		(LMH6626) R_L = 100 Ω		±4.3	±4.8		
			-40°C ≤ T_J ≤ 125°C	±4.2			
		(LMH6626) No Load		±4.8	±5.2		
			-40°C ≤ T_J ≤ 125°C	±4.65			
R_O	Output impedance	f ≤ 100 KHz			10		mΩ
I_{SC}	Output short circuit current	(LMH6624) Sourcing to Ground ΔV_{IN} = 200 mV (7)(8)		100	156		mA
			-40°C ≤ T_J ≤ 125°C	85			
		(LMH6624) Sinking to Ground ΔV_{IN} = −200 mV (7)(8)		100	156		
			-40°C ≤ T_J ≤ 125°C	85			
		(LMH6626) Sourcing to Ground ΔV_{IN} = 200 mV (7)(8)		65	120		
			-40°C ≤ T_J ≤ 125°C	55			
		(LMH6626) Sinking to Ground ΔV_{IN} = −200 mV(7)(8)		65	120		
			-40°C ≤ T_J ≤ 125°C	55			
I_{OUT}	Output current	(LMH6624) Sourcing, V_O = +4.3 V Sinking, V_O = −4.3 V			100		mA
		(LMH6626) Sourcing, V_O = +4.3 V Sinking, V_O = −4.3 V			80		
POWER SUPPLY							
PSRR	Power supply rejection ratio	V_S = ±5.4 V to ±6.6 V		82	88		dB
			-40°C ≤ T_J ≤ 125°C	80			
I_S	Supply current (per channel)	No Load			12	16	mA
			-40°C ≤ T_J ≤ 125°C			18	

(7) Applies to both single-supply and split-supply operation. Continuous short circuit operation at elevated ambient temperature can result in exceeding the maximum allowed junction temperature of 150°C.
(8) Short circuit test is a momentary test. Output short circuit duration is 1.5 ms.

Appendix 4

ANALOG DEVICES

250 MHz, Voltage Output, 4-Quadrant Multiplier

AD835

FEATURES

- Simple: basic function is W = XY + Z
- Complete: minimal external components required
- Very fast: Settles to 0.1% of full scale (FS) in 20 ns
- DC-coupled voltage output simplifies use
- High differential input impedance X, Y, and Z inputs
- Low multiplier noise: 50 nV/√Hz

APPLICATIONS

- Very fast multiplication, division, squaring
- Wideband modulation and demodulation
- Phase detection and measurement
- Sinusoidal frequency doubling
- Video gain control and keying
- Voltage-controlled amplifiers and filters

FUNCTIONAL BLOCK DIAGRAM

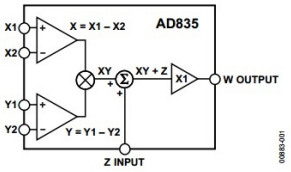

Figure 1.

Figure 5.3: Datasheet Multiplier AD835

SPECIFICATIONS

T_A = 25°C, V_S = ±5 V, R_L = 150 Ω, C_L ≤ 5 pF, unless otherwise noted.

Table 1.

Parameter	Conditions	Min	Typ	Max	Unit
TRANSFER FUNCTION			$W = \frac{(X1-X2)(Y1-Y2)}{U} + Z$		
INPUT CHARACTERISTICS (X, Y)					
Differential Voltage Range	V_{CM} = 0 V		±1		V
Differential Clipping Level		±1.2[1]	±1.4		V
Low Frequency Nonlinearity	X = ±1 V, Y = 1 V		0.3	0.5[1]	% FS
	Y = ±1 V, X = 1 V		0.1	0.3[1]	% FS
vs. Temperature	T_{MIN} to T_{MAX}[2]				
	X = ±1 V, Y = 1 V			0.7	% FS
	Y = ±1 V, X = 1 V			0.5	% FS
Common-Mode Voltage Range		−2.5		+3	V
Offset Voltage			±3	±20[1]	mV
vs. Temperature	T_{MIN} to T_{MAX}[2]			±25	mV
CMRR	f ≤ 100 kHz; ±1 V p-p	70[1]			dB
Bias Current			10	20[1]	μA
vs. Temperature	T_{MIN} to T_{MAX}[2]			27	μA
Offset Bias Current			2		μA
Differential Resistance			100		kΩ
Single-Sided Capacitance			2		pF
Feedthrough, X	X = ±1 V, Y = 0 V			−46[1]	dB
Feedthrough, Y	Y = ±1 V, X = 0 V			−60[1]	dB
DYNAMIC CHARACTERISTICS					
−3 dB Small Signal Bandwidth		150	250		MHz
−0.1 dB Gain Flatness Frequency			15		MHz
Slew Rate	W = −2.5 V to +2.5 V		1000		V/μs
Differential Gain Error, X	f = 3.58 MHz		0.3		%
Differential Phase Error, X	f = 3.58 MHz		0.2		Degrees
Differential Gain Error, Y	f = 3.58 MHz		0.1		%
Differential Phase Error, Y	f = 3.58 MHz		0.1		Degrees
Harmonic Distortion	X or Y = 10 dBm, second and third harmonic				
	Fund = 10 MHz		−70		dB
	Fund = 50 MHz		−40		dB
Settling Time, X or Y	To 0.1%, W = 2 V p-p		20		ns
SUMMING INPUT (Z)					
Gain	From Z to W, f ≤ 10 MHz	0.990	0.995		
−3 dB Small Signal Bandwidth			250		MHz
Differential Input Resistance			60		kΩ
Single-Sided Capacitance			2		pF
Maximum Gain	X, Y to W, Z shorted to W, f = 1 kHz		50		dB
Bias Current			50		μA

Appendix 5

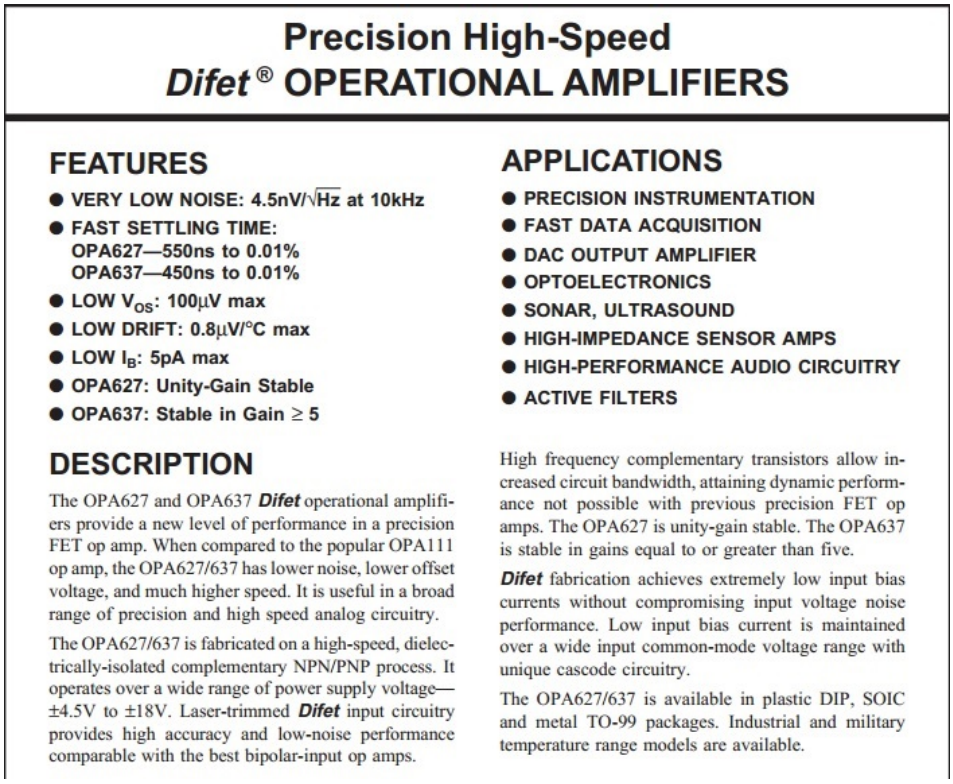

Precision High-Speed *Difet*® OPERATIONAL AMPLIFIERS

FEATURES

- VERY LOW NOISE: 4.5nV/√Hz at 10kHz
- FAST SETTLING TIME:
  OPA627—550ns to 0.01%
  OPA637—450ns to 0.01%
- LOW V_{OS}: 100μV max
- LOW DRIFT: 0.8μV/°C max
- LOW I_B: 5pA max
- OPA627: Unity-Gain Stable
- OPA637: Stable in Gain ≥ 5

APPLICATIONS

- PRECISION INSTRUMENTATION
- FAST DATA ACQUISITION
- DAC OUTPUT AMPLIFIER
- OPTOELECTRONICS
- SONAR, ULTRASOUND
- HIGH-IMPEDANCE SENSOR AMPS
- HIGH-PERFORMANCE AUDIO CIRCUITRY
- ACTIVE FILTERS

DESCRIPTION

The OPA627 and OPA637 ***Difet*** operational amplifiers provide a new level of performance in a precision FET op amp. When compared to the popular OPA111 op amp, the OPA627/637 has lower noise, lower offset voltage, and much higher speed. It is useful in a broad range of precision and high speed analog circuitry.

The OPA627/637 is fabricated on a high-speed, dielectrically-isolated complementary NPN/PNP process. It operates over a wide range of power supply voltage—±4.5V to ±18V. Laser-trimmed ***Difet*** input circuitry provides high accuracy and low-noise performance comparable with the best bipolar-input op amps.

High frequency complementary transistors allow increased circuit bandwidth, attaining dynamic performance not possible with previous precision FET op amps. The OPA627 is unity-gain stable. The OPA637 is stable in gains equal to or greater than five.

Difet fabrication achieves extremely low input bias currents without compromising input voltage noise performance. Low input bias current is maintained over a wide input common-mode voltage range with unique cascode circuitry.

The OPA627/637 is available in plastic DIP, SOIC and metal TO-99 packages. Industrial and military temperature range models are available.

Figure 5.4: Datasheet Operational Amplifier opa627

SPECIFICATIONS

ELECTRICAL

At T_A = +25°C, and V_S = ±15V, unless otherwise noted.

PARAMETER	CONDITIONS	OPA627BM, BP, SM OPA637BM, BP, SM MIN	TYP	MAX	OPA627AM, AP, AU OPA637AM, AP, AU MIN	TYP	MAX	UNITS
OFFSET VOLTAGE (1)								
Input Offset Voltage			40	100		130	250	µV
AP, BP, AU Grades			100	250		280	500	µV
Average Drift			0.4	0.8		1.2	2	µV/°C
AP, BP, AU Grades			0.8	2		2.5		µV/°C
Power Supply Rejection	V_S = ±4.5 to ±18V	106	120		100	116		dB
INPUT BIAS CURRENT (2)								
Input Bias Current	V_{CM} = 0V		1	5		2	10	pA
Over Specified Temperature	V_{CM} = 0V			1			2	nA
SM Grade	V_{CM} = 0V			50				nA
Over Common-Mode Voltage	V_{CM} = ±10V		1			2		pA
Input Offset Current	V_{CM} = 0V		0.5	5		1	10	pA
Over Specified Temperature	V_{CM} = 0V			1			2	nA
SM Grade				50				nA
NOISE								
Input Voltage Noise								
Noise Density: f = 10Hz			15	40		20		nV/√Hz
f = 100Hz			8	20		10		nV/√Hz
f = 1kHz			5.2	8		5.6		nV/√Hz
f = 10kHz			4.5	6		4.8		nV/√Hz
Voltage Noise, BW = 0.1Hz to 10Hz			0.6	1.6		0.8		µVp-p
Input Bias Current Noise								
Noise Density, f = 100Hz			1.6	2.5		2.5		fA/√Hz
Current Noise, BW = 0.1Hz to 10Hz			30	60		48		fAp-p
INPUT IMPEDANCE								
Differential			10^{13} || 8			*		Ω || pF
Common-Mode			10^{13} || 7			*		Ω || pF
INPUT VOLTAGE RANGE								
Common-Mode Input Range		±11	±11.5		*	*		V
Over Specified Temperature		±10.5	±11		*	*		V
Common-Mode Rejection	V_{CM} = ±10.5V	106	116		100	110		dB
OPEN-LOOP GAIN								
Open-Loop Voltage Gain	V_O = ±10V, R_L = 1kΩ	112	120		106	116		dB
Over Specified Temperature	V_O = ±10V, R_L = 1kΩ	106	117		100	110		dB
SM Grade	V_O = ±10V, R_L = 1kΩ	100	114					dB
FREQUENCY RESPONSE								
Slew Rate: OPA627	G = –1, 10V Step	40	55		*	*		V/µs
OPA637	G = –4, 10V Step	100	135		*	*		V/µs
Settling Time: OPA627 0.01%	G = –1, 10V Step		550			*		ns
0.1%	G = –1, 10V Step		450			*		ns
OPA637 0.01%	G = –4, 10V Step		450			*		ns
0.1%	G = –4, 10V Step		300			*		ns
Gain-Bandwidth Product: OPA627	G = 1		16			*		MHz
OPA637	G = 10		80			*		MHz
Total Harmonic Distortion + Noise	G = +1, f = 1kHz		0.00003			*		%
POWER SUPPLY								
Specified Operating Voltage			±15			*		V
Operating Voltage Range		±4.5		±18	*		*	V
Current			±7	±7.5		*	*	mA
OUTPUT								
Voltage Output	R_L = 1kΩ	±11.5	±12.3		*	*		
Over Specified Temperature		±11	±11.5		*	*		V
Current Output	V_O = ±10V		±45			*		mA
Short-Circuit Current		±35	+70/–55	±100	*	*	*	mA
Output Impedance, Open-Loop	1MHz		55			*		Ω
TEMPERATURE RANGE								
Specification: AP, BP, AM, BM, AU		–25		+85	*		*	°C
SM		–55		+125				°C
Storage: AM, BM, SM		–60		+150	*		*	°C
AP, BP, AU		–40		+125	*		*	°C
θ_{J-A}: AM, BM, SM			200			*		°C/W
AP, BP			100			*		°C/W
AU			160					°C/W

* Specifications same as "B" grade.

NOTES: (1) Offset voltage measured fully warmed-up. (2) High-speed test at T_J = +25°C. See Typical Performance Curves for warmed-up performance.

Bibliography

[1] Your health, your choices. (n.d.). Retrieved December 10, 2014, from http://www.nhs.uk

[2] Asthma UK — Home. (n.d.). Retrieved December 12, 2014, from http://www.asthma.org.uk

[3] Swindle, E., Collins, J., and Davies, D. (2009). Breakdown in epithelial barrier function in patients with asthma: Identification of novel therapeutic approaches. *Journal of Allergy and Clinical Immunology*, 124(1), 23-34 quiz 35-6.

[4] C. P. d. Schans, Respir. Care, 2007, 52, 1150-1156.

[5] Diamond, J. M. (2007). The Ephitelial Junction: Bridge, Gate, and Fence. *Twenty-first Bowditch lecture*, 1997, Los Angeles, California.

[6] Sun, T., Swindle, E., Collins, J., Holloway, J., Davies, D., and Morgan, H. (2010). On-chip epithelial barrier function assays using electrical impedance spectroscopy. *Lab on a Chip*, 10(12), 1611-1611.

[7] Sangeeta N. Bhatia, Donald E. Ingber (2014). Microfluidic organs-on-chips. *Nature Biotechnology* 32, 760-772.

[8] Mathieu Odijk, Andries D. van der Meer, Daniel Levner, Hyun Jung Kim, Marinke W. van der Helm, Loes I. Segerink, Jean-Phillipe Frimat, Geraldine A. Hamilton, Donald E. Ingberb and Albert van den Berga (2014). Measuring direct current trans-epithelial electrical resistance in organ-on-a-chip microsystems. *Lab Chip*, 5(3), 745-52.

[9] Gunzel, D. K., S. M.; Rosenthal, R.; Fromm, M. (2010). Biophysical Methods to Study Tight Junction Permeability *Current Topics in Membranes*, 65, 39-78.

[10] Wegener, J., and Seebach, J. (2014). Experimental tools to monitor the dynamics of endothelial barrier function: A survey of in vitro approaches. *Cell and Tissue Research*, 355(3), 485-514.

[11] Rothen-Rutishauser, B., Riesen, F., Braun, A., GÃ¼nthert, M., and Wunderli-Allenspach, H. (2002). Dynamics of Tight and Adherens Junctions Under EGTA Treatment. *Journal of Membrane Biology*, 188(2), 151-162.

[12] Guttman, J., and Finlay, B. (2009). Tight junctions as targets of infectious agents. *Biochimica Et Biophysica Acta (BBA) - Biomembranes*, 1788(4), 832-841.

[13] M. Tartagni (2014). *IONIC TRANSDUCTION and IMPEDANCE SPECTROSCOPY*. Presentation slides for the course Sensori e nanotecnologie, University of Bologna, Department of Electrical, Electronic and Information Engineering

[14] Ateh, D., Waterworth, A., Walker, D., Brown, B., Navsaria, H., and Vadgama, P. (2007). Impedimetric sensing of cells on polypyrrole-based conducting polymers. *Journal of Biomedical Materials Research Part A*, 83(2), 391-400.

[15] Malleo, D., Nevill, J., Ooyen, A., Schnakenberg, U., Lee, L., and Morgan, H. (2010). Characterization of electrode materials for dielectric spectroscopy. *Review of Scientific Instruments*, 81, 016104.

[16] B. ILIC, D. CZAPLEWSKI, P. NEUZIL, T. STANCZYK, J. BLOUGH, G. J. MACLAY (2000). Preparation and characterization of platinum black electrodes. *Kluwer Academic Publishers*, 35, 3447-3457.

[17] P. Ellappan, R. Sundararajan (2015). A simulation study of the electrical model of a biologic cell. *Journal of Electronics* 63, 297-307.

[18] Michele Rossi, Marco Bennati, Federico Thei, and Marco Tartagni (2012). A Low-cost and Portable System for Real-time Impedimetric Measurements and Impedance Spectroscopy of Sensors. *SENSORDEVICES*, 2308-3514.

[19] M. Tartagni (2014). *SENSOR INTERFACES*. Presentation slides for the course Sensori e nanotecnologie, University of Bologna, Department of Electrical, Electronic and Information.

[20] M. Tartagni (2014). *NOISE*. Presentation slides for the course Sensori e nanotecnologie, University of Bologna, Department of Electrical, Electronic and Information.

[21] P. T. Patil, G. K. Mukherjee, A. K. Sharma and R. R. Mudholkar. (2009). High-Gain Transimpedance Amplifier (TIA) for Night Airglow Photometer. *International Journal of Electronic Engineering Research*, 1(2), 109-116.

[22] Weidong Gong (2010). *Ocean Sensors for marine environmental monitoring*. Doctoral Thesis, University of Southampton , School of Electronics and Computer Science.

List of Figures

1.1 Images showing the immunofluorescent staining of the tight junction protein ZO-1 in the epithelial cell monolayers, treated with EGTA at the concentrations indicated. (a) Control cell monolayer, (b) 1mM EGTA treatment, (c) 5mM EGTA treatment, (d) 10mM EGTA treatment [6] 2
1.2 3D assembly structure of the Bio-impedance chip [6] . . 4
1.3 The cell monolayers were treated with different concentrations of TX-100 and EGTA. The data show the disruption in the epithelial cell barrier function [6] . . . 5
1.4 Organ-on-Chip [8] 6
1.5 TEER measurements for the Organ-on-a-chip and Transwell using human intestinal epithelial Caco-2 cells [8] . 7
1.6 Microfluidics Design Biochip 9

2.1 Epithelial cell culture Biochip 12
2.2 Equivalent circuit model of the system for extracting the electrical properties of the epithelia cell (a), (b) simplified model 14
2.3 Chopstick Electrodes and Transwell 17
2.4 Electrical Resistance System 18
2.5 Magnitude (top) and Phase (bottom) of the Biochip Impedance by Matlab Simulation 21

3.1 General representation of the double layer formed at the metal electrolyte interface [13] 24
3.2 Potential profile in the double layer formed at a metallic electrode charged negatively [13] 25

3.3 Double Layer Capacitance [13] 27
3.4 Magnitude (Top) and Phase (Bottom) of the biochip impedance with Double Layer Effect 29
3.5 Equivalent Circuit Model of the biochip without cells monolayer 30
3.6 Fitting to estimate the value of the double layer capacitance 31
3.7 Dot Ring and Straight Electrodes 33
3.8 Impedance magnitude (a) and phase (b) for bright platinum, Pt black, IrOx and PPy/PSS-coated electrodes [15] 35
3.9 Set-up for the Electrochemical deposition of Pt 37
3.10 Image Coated Electrodes (Top) and Images Coated Electrodes under the microscope (Bottom) 38
3.11 Equivalent Circuit Model of the biochip without cells monolayer with coated electrodes 39
3.12 Fitting to estimate the value of the double layer capacitance when the electrodes are coated 40
3.13 Typical applied voltage to electrochemical cell (blue line) and related flowing current (red line) 41
3.14 Novocontrol Alpha-n high resolution dielectric analyzer 42
3.15 Magnitude (Top) and Phase (Bottom) of the biochip impedance with coated electrodes and uncoated electrodes 44
3.16 Magnitude (Top) and Phase (Bottom) of the Biochip Impedance without cells , for the Dot and Ring electrodes, with Double Layer Effect and medium flow rate of 7ul/hr 47
3.17 Magnitude (Top) and Phase (Bottom) of the Biochip Impedance without cells, for the Dot and Ring electrodes, with Double Layer Effect and medium flow rate of 30ml/hr 48
3.18 Magnitude (Top) and Phase (Bottom) of the Biochip Impedance without cells, for the Dot and Ring electrodes, with Double Layer Effect and medium flow rate of 800ml/hr 49

3.19 Magnitude (Top) and Phase (Bottom) of the Biochip Impedance without cells, for the Dot and Ring electrodes, with Double Layer Effect and medium conductivity of 30mS/cm 51
3.20 Magnitude (Top) and Phase (Bottom) of Biochip Impedance without cells, for the Dot and Ring electrodes, with Apical, with Double Layer Effect and medium flow rate of 30ml/hr 52
3.21 Magnitude (Top) and Phase (Bottom) of the Biochip Impedance without cells, for the Straigth Electrodes, with Double Layer Effect, medium flow rate of 30ml/hr 53
3.22 Magnitude (Top) and Phase (Bottom) of the Biochip Impedance without cells, for the Dot and Ring Electrodes, no Double Layer Effect and medium flow rate of 30ml/hr 55
3.23 Magnitude (Top) and Phase (Bottom) of the Biochip Impedance without cells, for the Dot and Ring Electrodes, with Apical, no Double layer Effect and medium flow rate of 30ml/hr 56
3.24 Magnitude (Top) and Phase (Bottom) of the Biochip Impedance without cells, for the Straigth Electrodes, no Double Layer Effect and medium flow rate of 30ml/hr 57
3.25 Magnitude of the Biochip Impedance without cells, for the Dot and Ring electrodes, no Double Layer Effect and medium flow rate of 30ul/hr 59
3.26 Relation between Magnitude of the biochip impedance and conductivity of the medium. Fitting DATA, R-Squared = 0.95 59

4.1 Lock-in principle [19] 62
4.2 Lock-in principle in frequency domain [19] 64
4.3 Complex impedance detection by Lock-in amplifier [19] 68
4.4 PCB Top-layer Lock-in amplifier 72
4.5 Bill of materials 73
4.6 Block Diagram of the PCB 75

4.7 Schematic circuit of the Multiplexer ADG726. In this figure there are also the Headers that are connected with the Multiplexer as the Header for the DAQ (Header 9), the Header relative to the input signals (Header 7) and that one for the output signals (Header 8 and Header 9) 76
4.8 Part of a DAQ system 77
4.9 Biochip equivalent circuit model and schematic circuit Transimpedance 80
4.10 Schematic circuit Amplifier inverting 80
4.11 op-gain-IN: output signal from transimpedance, op-gain-OUT: output signal from amplifier inverting 81
4.12 Phase of the output signals from Multipliers 82
4.13 Schematic circuit Multipliers 83
4.14 Output signals from the multipliers 83
4.15 Schematic circuit Filters 84
4.16 DC output 85
4.17 Equivalent circuit model ZView 87
4.18 Equivalent circuit model ZView without cells 87
4.19 Bottom Layer PCB: Capacitive Decoupling 88
4.20 Piece Interface 91
4.21 PCB design connect to biochip 91

5.1 Datasheet Multiplexer ADG726 99

5.2 Datasheet Operational Amplifier LMH6624 103

5.3 Datasheet Multiplier AD835 107

5.4 Datasheet Operational Amplifier opa627 109

Acknowledgements

First of all, I would like to thank advisor Prof. Marco Tartagni, for his support and encouragement to begin this experience. I would like to thank Prof. Hywel Morgan for giving me the opportunity to conclude my studies in Southampton.

I would like to thank Ing. Riccardo Reale for his help and support during these six months. I would like to thank Dr. Daniel Spencer for his help in the lab. I would like to thank all the members of the Nano Research Group.

A very important thanks all my family for their unconditional love and encouragement. I would also like to thank all my friends.